This article has been accepted for inclusion in a future issue of this journal. Content is final as presented, with the exception of pagination.

Event-Triggered Fully Distributed Bipartite Containment Control for Multi-Agent Systems Under DoS Attacks and External Disturbances

Yanjun Zhao, Haibin Sun, *Member, IEEE*, Jun Yang, *Fellow, IEEE*, Linlin Hou, and Dong Yang, *Member, IEEE*

***Abstract*— This study investigates bipartite containment control algorithm for multi-agent systems which are vulnerable to DoS attacks and external disturbances. Disturbances are generated via a series of exogenous nonlinear systems with a one-sided Lipschitz condition. To estimate unknown system states and external disturbances, a set of decentralized state observers and disturbance observers is proposed. Then a fully distributed control protocol is adopted to avoid the utilization of global information. An attack compensator is introduced to mitigate the adverse impacts of DoS attacks. Furthermore, Zeno-free dynamic event-triggered mechanisms that do not require continuous communication between neighboring agents are presented to conserve limited communication resources. In the end, satellite flight systems are introduced to illustrate the feasibility of the designed control scheme.**

***Index Terms*— Bipartite containment, fully distributed, multi-agent systems, DoS attacks, external disturbances.**

I. Introduction

COLLABORATIVE control research of multi-agent systems (MASs) such as spacecraft formation flight [1] and smart grids [2], has received widespread interest recently. In the domain of cooperative control for MASs, containment control has attracted significant attention when multiple leaders are involved, such as cooperative transportation, hazardous material handling and fire rescue. In this framework, agents are categorized into followers and leaders, with the trajectories of the followers are contained within a convex hull consisting of multiple leaders [3]. For example, a group of autonomous vehicles is divided into two parts when performing a task, a part of autonomous vehicles (designated as leaders) equipped with necessary sensors to detect the hazardous obstacles and guide the another part of vehicles (designated as followers) from one target to another safely, by ensuring that the followers execute the primary task within the scope established by leaders. Distributed controllers were designed in [4], [5], and [6] to achieve containment control goals.

The aforementioned results mainly discussed the networks with non-negative weights, implying that the interactions between agents are only cooperative. By contrast, signed networks produce more complex dynamic characters than traditional networks by introducing competition interactions, such as bipartite consensus [7], [8], leader-following bipartite consensus [9], [10], and bipartite containment [11], [12], [13], [14], due to which they have several potential applications in many practical systems, e.g., unmanned aerial vehicles and economic systems. For instance, a cooperative/antagonistic interaction can represent to reflect a friend/foe, or trust/distrust relationship between nodes in social networks. Inspired by these facts, research on bipartite containment control problem in MASs holds significant theoretical and practical value.

Notably, the control schemes discussed in aforementioned studies need some global information, for example communication network structure. However, global information may not be available for practical situations. Correspondingly, a fully distributed control scheme is valued without any global information. Various fully distributed control protocols have been proposed. Fully distributed control strategies were proposed in the absence of the leader to achieve consensus in [15], [16], [17], and [18]. For a single leader, a fully distributed controller was designed in [19] to achieve both leaderless and leader-following consensus. Considering MASs with multiple leaders, fully distributed protocols were constructed to realize containment control [20] and bipartite containment control [21], [22].

These findings were obtained in a perfect network environment. However, the network topology of MASs is vulnerable and easily influenced by various network attacks, for instance, false data injection attacks (FDIAs) [23], [24] and denial-of-service (DoS) attacks [25], [26], [27], which may degrade the system performance. In particular, DoS attacks hinder the transmission of information between agents and are easy to launch by adversaries, which prevents the timely updating of control inputs, thereby affecting the system stability. Thus, the secure control problem for MASs under DoS attacks is significant and has become a focus problem [28], [29]. Notably, few studies have focused on achieving bipartite containment

Received 13 October 2024; revised 18 December 2024 and 13 January 2025; accepted 21 January 2025. This work was supported in part by the National Key Research and Development Program of China under Grant 2023YFB4706800; in part by the National Natural Science Foundation of China under Grant 62173205, Grant 62273254, and Grant 62273199; in part by Taishan Scholar Project of Shandong Province under Grant tsqn202306181, Grant tsqn202306191, and Grant tsqn202211132; and in part by the Natural Science Foundation of Shandong Province under Grant ZR2023MF049 and Grant ZR2024MF078. This article was recommended by Associate Editor Y. Tang. *(Corresponding author: Haibin Sun.)*

Yanjun Zhao, Haibin Sun, and Dong Yang are with the School of Engineering, Qufu Normal University, Rizhao, Shandong 276826, China (e-mail: 1215954259@qq.com; seusunhaibin@gmail.com; yangdong850901@126.com).

Jun Yang is with the Department of Aeronautical and Automotive Engineering, Loughborough University, LE11 3TU Loughborough, U.K. (e-mail: j.yang3@lboro.ac.uk).

Linlin Hou is with the School of Information Science and Engineering, Qufu Normal University, Rizhao, Shandong 276826, China (e-mail: houtingting8706@126.com).

Digital Object Identifier 10.1109/TCSI.2025.3534241

1549-8328 © 2025 IEEE. All rights reserved, including rights for text and data mining, and training of artificial intelligence and similar technologies. Personal use is permitted, but republication/redistribution requires IEEE permission.
See https://www.ieee.org/publications/rights/index.html for more information.
Authorized licensed use limited to: STAATS U UNIBIBL BREMEN. Downloaded on March 16,2025 at 11:30:45 UTC from IEEE Xplore. Restrictions apply.

This article has been accepted for inclusion in a future issue of this journal. Content is final as presented, with the exception of pagination.

under fully distributed controllers for MASs with DoS attacks, which is the research motivation for this paper.

Another challenge is that the network communication bandwidth is limited in MASs. Traditional time-triggered mechanisms inevitably produce redundant data, which leads to network congestion. To overcome this difficulty, event-triggered mechanisms (ETMs) were proposed to save resources [30], [31]. Therefore, many results have been obtained for MASs through ETMs [32], [33]. In particular, when MASs are subjected to DoS attacks, some secure consensus protocols were developed via ETMs [34], [35], [36].

Nevertheless, measuring the all system states in practical scenarios is often difficult (unattainable or too costly) [37]. Consequently, observer-based control is considered, e.g., reduced-order observer-based bipartite tracking control for MASs discussed in [38] and the fuzzy observer-based bipartite containment control problem for MASs explored in [39]. Moreover, these systems are inevitably affected by external disturbances, which may influence the control performance of closed-loop systems. The adverse effects typically manifest as reduced system stability, increased control errors, slower response speed, and diminished control accuracy. Owing to the requirement for high performance and precision, disturbance compensation control methods have gained widespread acceptance. For instance, consensus and bipartite average tracking problem in MASs with bounded external disturbances was integrated in [40] and [41], the problem of bipartite consensus of nonlinear MASs based on a disturbance observer was addressed in [42], finite-time leader-following consensus in MASs subjected to external disturbances was investigated in [43] and an observer-based composite anti-disturbance controller was constructed for MASs in [44]. However, MASs are susceptible to disturbance from physical layer and cyber attacks from cyber layer simultaneously. Hence it is necessary to developed control scheme to guarantee that MASs have good anti-disturbance and anti-attack performance.

For a class of MASs impacted by DoS attacks and external disturbances, this paper designs a fully distributed controller based on dynamic ETMs to achieve bipartite containment. An attack compensator is introduced to mitigate the effects of DoS attacks. Additionally, the observers are given to estimate the system states and external disturbances. Notably, when both DoS attacks and disturbances coexist, it is difficult to design a appropriate controller to realize anti-disturbance and anti-attack performance simultaneously, thus how to reduce the influence of DoS attacks and disturbances is a challenge addressed in this paper. Furthermore, how to design fully distributed control schemes including controller and ETMs to avoid using global information of the topology structure is other challenge of this paper. The primary contributions of this paper are as follows:

- An adaptive law with a projection operator is presented to design a fully distributed bipartite containment control protocol. Unlike existing results that employ the Laplacian matrix of topology structure [11], [12], [13], [14], our control method avoids the use of global information. In addition, it differs from previous fruits that do not refer to DoS attacks [21], [22], and our proposed protocol still works well in existing DoS attacks.
- A decentralized state observer is presented to estimate the unknown followers' states. According to whether DoS attacks exists, two ETMs are constructed for unreliable communication network. When DoS attacks occur during the sleep period, an ETM is designed based on the neighbors' estimation states; otherwise, the neighbors' estimation states will not be used. An attack compensator is constructed to reconstruct the neighbors' states. Subsequently, another ETM is proposed based on the states of the compensator. In comparison to existing studies with DoS attacks for MASs [34], no global information is introduced in the triggering function. Further, a dynamic variable is included to reduce the triggering frequency.
- In contrast to the existing anti-disturbance control scheme for MASs [40], [41], [42], [43], [44], this paper gives a set of novel exogenous systems to describe disturbance signals, where the dynamic system and output equation are simultaneously subjected to nonlinear functions satisfying a one-sided Lipschitz condition. This can be used to model wider disturbances. To eliminate the impact of external disturbances, a disturbance observer is designed using output information, and a disturbance estimation value is incorporated into the distributed containment control scheme to improve anti-disturbance performance.

Notations: $1_p = [1, \cdots, 1]^T \in \mathbb{R}^p$ is a $p \times 1$-dimension column vector. $I_M \in \mathbb{R}^{M\times M}$ is an $M \times M$-dimension identity matrix. $|a_{ih}| = \text{sgn}(a_{ih})a_{ih}$ with $\text{sgn}(\cdot)$ is a sign function. $A > 0$ represents that A is a positive definite matrix. $\otimes$ is the Kronecker product.

II. Preliminaries and Problem Formulation

A. Preliminaries

1) Graph Theory: Graph $\mathcal{G} = (\mathcal{V}, \mathcal{E}, \mathcal{A})$ denotes the communication topology between agents, where $\mathcal{V}$ is the vertex set, $\mathcal{E}$ is the edge set, $\mathcal{A} = (a_{ih}) \in \mathbb{R}^{M\times M}$ is the adjacency matrix. The undirected graph indicates that information can be transferred between two agents, namely $i \leftrightarrow h$. If $h \to i$, agent h is referred to as a neighbor of agent i, and the neighbor set of agent i is expressed as $N_i = \{h|(h, i) \in \mathcal{E}\}$. This paper assumes that there is no closed loop, i.e. $a_{ii} = 0$. The Laplacian matrix corresponding to graph $\mathcal{G}$ is denoted as $\mathcal{L} = \mathcal{C} - \mathcal{A}$, where $\mathcal{C}$ is a diagonal matrix with elements $\sum_{h\in\mathcal{N}_i} |a_{ih}|$. Moreover, this paper supposes that the graph $\mathcal{G}$ is structurally balanced, that is, there exist a bipartition $\{\mathcal{V}^{(1)}, \mathcal{V}^{(2)}\}$ of $\mathcal{V}$ such that $\mathcal{V}^{(1)} \vee \mathcal{V}^{(2)} = \mathcal{V}$ and $\mathcal{V}^{(1)} \wedge \mathcal{V}^{(2)} = \emptyset$, with the following relationship: $a_{ih} \geq 0, i, h \in \mathcal{V}^{(J)}$ and $a_{ih} \leq 0, i \in \mathcal{V}^{(J)}, j \in \mathcal{V}^{(3-J)}, J \in \{1, 2\}$.

Assumption 1 [20]: Each follower receives information from at least one leader, while the leaders have no neighbors.

2) DoS Attacks Model: Usually, attackers with limited energy select to lunch intermittent DoS attacks on the communication network of the system, and they will terminate attacks at intervals and keep sleeping to conserve energy for subsequent DoS attacks. The n^{th} DoS attack activate interval is defined as $\left[T_n^{\text{on}}, T_n^{\text{off}}\right)$, and the n^{th} DoS attack sleep interval is defined as $\left[T_{n-1}^{\text{off}}, T_n^{\text{on}}\right)$. The total activate duration of DoS attacks within the interval $[0, t]$ is expressed as $\Omega_a(0, t) = \left\{\bigcup_{n\in\mathbb{N}} \left[T_n^{\text{on}}, T_n^{\text{off}}\right)\right\} \bigcap [0, t]$, and the total sleeping duration is $\Omega_s(0, t) = [0, t] \backslash \Omega_a(0, t)$.

The acknowledgment (ACK) character technique is employed to judge whether the data is transmitted correctly or not in [25], in which the ACK signal is prioritized highest and its transmission delay can be ignored. Specifically, an ACK signal of $\delta(ACK) = 0$ indicates the absence of DoS attacks and successful communication with the agents. Conversely,

Authorized licensed use limited to: STAATS U UNIBIBL BREMEN. Downloaded on March 16,2025 at 11:30:45 UTC from IEEE Xplore. Restrictions apply.

This article has been accepted for inclusion in a future issue of this journal. Content is final as presented, with the exception of pagination.

$\delta(ACK) = 1$ represents a communication disruption caused by DoS attacks. Hence, the ACK signal can be used to represent DoS attack behavior, that is:

$$\delta(ACK) = \begin{cases} 0, & \text{no DoS attacks;} \\ 1, & \text{under DoS attacks.} \end{cases} \tag{1}$$

Assumption 2 [45]: For the total activate duration $|\Omega_a(0,t)|$ of DoS attacks in $[0,t]$, suppose

$$|\Omega_a(0,t)| \leq \Omega_0 + \frac{t}{\tau_a}, \tag{2}$$

where $\tau_a > 1$, $\Omega_0 > 0$ is a constant.

Remark 1: Considering the attack energy restricted and self-repairing capability of systems, Assumption 2 is reasonable in practice, which indicates that the total activation duration of DoS attacks is limited.

B. Problem Formulation

Consider a linear MAS comprising M followers and $N-M$ leaders, which the followers are labeled as $1, 2, \cdots, M$, and the leaders are labeled as $M+1, M+2, \cdots, N$. The dynamic of the i^{th} follower is:

$$\begin{aligned} \dot{x}_i(t) &= Ax_i(t) + B[u_i(t) + d_i(t)], \\ y_i(t) &= Cx_i(t), \ i = 1, \cdots, M, \end{aligned} \tag{3}$$

where $x_i(t) \in \mathbb{R}^n$, $u_i(t) \in \mathbb{R}^m$, and $y_i(t) \in \mathbb{R}^p$ are the state, control input, and output of agent i, respectively, A, B, C are constant matrices with appropriate dimensions, $d_i(t) \in \mathbb{R}^m$ is an external disturbance with the following dynamic:

$$\begin{aligned} \dot{\omega}_i(t) &= W\omega_i(t) + F_1 f_{01}(\omega_i(t)), \\ d_i(t) &= V\omega_i(t) + F_2 f_{02}(\omega_i(t)), \ i = 1, \cdots, M, \end{aligned} \tag{4}$$

where $\omega_i(t) \in \mathbb{R}^q$ is the unknown state vector, $f_{01}(\omega_i(t))$ and $f_{02}(\omega_i(t))$ are nonlinear functions with known structure and satisfy the one-sided Lipschitz condition. W, V, F_1, F_2 are constant matrices.

Remark 2: The nonlinear exogenous systems (4) can be used to describe a broader range of disturbances. For example, it reduces to a linear exogenous system when $f_{01}(\omega_i(t)) = f_{02}(\omega_i(t)) = 0$, as illustrated in Fig. 1(a). Furthermore, various nonlinear functions are presented to generate many types of disturbance signals, as depicted in Fig. 1(b), (c) and (d). Especially, if a nonlinearity is Lipschitz, it satisfies the one-sided Lipschitz condition, but the reverse is not necessarily true.

The dynamic of l^{th} leader is:

$$\begin{aligned} \dot{x}_l(t) &= Ax_l(t), \\ y_l(t) &= Cx_l(t), \ l = M+1, \cdots, N, \end{aligned} \tag{5}$$

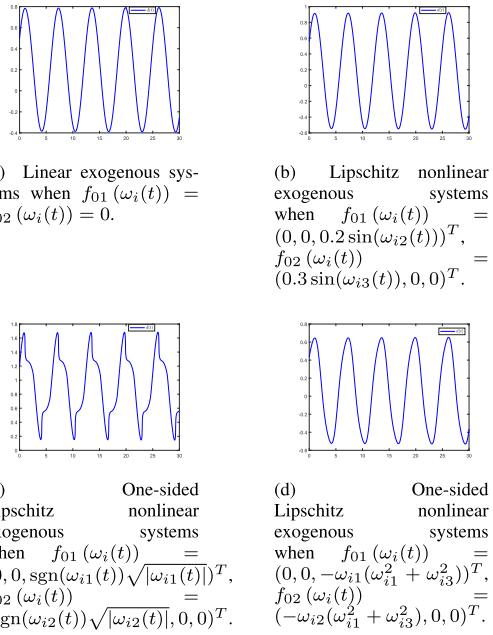
where $x_l(t) \in \mathbb{R}^n$ and $y_l(t) \in \mathbb{R}^p$ are the state and output of the leader l, respectively.

Graph $\hat{\mathcal{G}} = (\hat{\mathcal{V}}, \hat{\mathcal{E}}, \hat{\mathcal{A}})$ represents the communication topology with all leaders and followers, and the following relationships hold:

$$\begin{aligned} &\hat{\mathcal{V}} = \mathcal{V} \cup \{M+1, \cdots, N\}, \ \hat{\mathcal{E}} \subseteq \hat{\mathcal{V}} \times \hat{\mathcal{V}}, \\ &\hat{\mathcal{A}} = \begin{bmatrix} 0_{(N-M)\times(N-M)} & 0_{(N-M)\times M} \\ \mathcal{A}_{\mathcal{FL}} & \mathcal{A}_{\mathcal{F}} \end{bmatrix}, \end{aligned}$$

where $\mathcal{A}_{\mathcal{F}}$ stands for the adjacency matrix of the leaderless graph $\mathcal{G}$, and $\mathcal{A}_{\mathcal{FL}}$ represents adjacency weight matrix between leaders and followers. Furthermore, the Laplacian matrix corresponding to graph $\hat{\mathcal{G}}$ is

$$\hat{\mathcal{L}} = \begin{bmatrix} 0_{(N-M)\times(N-M)} & 0_{(N-M)\times M} \\ L_2 & L_1 \end{bmatrix},$$



(a) Linear exogenous systems when $f_{01}(\omega_i(t)) = f_{02}(\omega_i(t)) = 0$.

(b) Lipschitz nonlinear exogenous systems when $f_{01}(\omega_i(t)) = (0, 0, 0.2\sin(\omega_{i2}(t)))^T$, $f_{02}(\omega_i(t)) = (0.3\sin(\omega_{i3}(t)), 0, 0)^T$.

(c) One-sided Lipschitz nonlinear exogenous systems when $f_{01}(\omega_i(t)) = (0, 0, \mathrm{sgn}(\omega_{i1}(t))\sqrt{|\omega_{i1}(t)|})^T$, $f_{02}(\omega_i(t)) = (\mathrm{sgn}(\omega_{i2}(t))\sqrt{|\omega_{i2}(t)|}, 0, 0)^T$.

(d) One-sided Lipschitz nonlinear exogenous systems when $f_{01}(\omega_i(t)) = (0, 0, -\omega_{i1}(\omega_{i1}^2 + \omega_{i3}^2))^T$, $f_{02}(\omega_i(t)) = (-\omega_{i2}(\omega_{i1}^2 + \omega_{i3}^2), 0, 0)^T$.

Fig. 1. Curves of $d_i(t)$.

where $L_2 = -\mathcal{A}_{\mathcal{FL}} \in \mathbb{R}^{M\times M}$, and $L_1 = \mathcal{L}_{\mathcal{F}} + \Pi_{\mathcal{FL}} \in \mathbb{R}^{M\times(N-M)}$ represents the interaction between leaders and followers, with $\Pi_{\mathcal{FL}} \in \mathbb{R}^{M\times(N-M)} = \mathrm{diag}\{\sum_{h=1}^{M}|a_{1h}|, \cdots, \sum_{h=1}^{M}|a_{Mh}|\}$.

Lemma 1 ([12]): Based on Assumption 1, SL_1S is an M-matrix with $S = \mathrm{diag}\{s_1, s_2, \cdots, s_M\}$ and $s_i = \pm 1$. Additionally, the sum of each row of $-SL_1^{-1}SL_2$ is one.

Assumption 3 [46]: $f(\cdot)$ satisfies one-sided Lipschitz and quadratic inner-bounded conditions, that is,

$$\begin{aligned} &\langle f(x_{\mu 1}) - f(x_{\mu 2}), x_{\mu 1} - x_{\mu 2}\rangle \leq \gamma_1 \|x_{\mu 1} - x_{\mu 2}\|^2, \\ &(f(x_{\mu 1}) - f(x_{\mu 2}))^T (f(x_{\mu 1}) - f(x_{\mu 2})) \leq \gamma_2 \|x_{\mu 1} - x_{\mu 2}\|^2 \\ &\quad + \gamma_3 \langle f(x_{\mu 1}) - f(x_{\mu 2}), x_{\mu 1} - x_{\mu 2}\rangle \end{aligned} \tag{6}$$

with $\gamma_1, \gamma_2, \gamma_3$ are scalars, and $x_{\mu 1}, x_{\mu 2} \in \mathbb{R}^n$.

Lemma 2 ([9]): For $x \in \mathbb{R}^{o_1}$, $y \in \mathbb{R}^{o_2}$ and a constant matrix $U_1 \in \mathbb{R}^{o_1\times o_2}$. There is a scalar $\rho > 0$ and a matrix $U_2 > 0 \in \mathbb{R}^{o_2\times o_2}$, the following inequality holds:

$$2\, x^T U_1 y \leq \rho x^T U_1 U_2 U_1^T x + \rho^{-1} y^T U_2^{-1} y.$$

Definition 1 ([20]): For any initial state $x_i(0)$, the systems (2)-(4) achieve bipartite containment if the bipartite containment error $e(t) = x_F(t) + \left(L_1^{-1}SL_2 \otimes I_{N-M}\right) x_L(t)$ remains uniformly bounded. Specifically, $e(t)$ satisfies

$$\{e(t) | \ \|e(t)\| \leq \aleph\},$$

where $\aleph$ is a positive constant.

The primary aim of this study is to develop a fully distributed controller with dynamic ETMs to achieve bipartite containment of MASs affected by DoS attacks and external disturbances. Fig. 2 exhibits the structure of MASs with DoS attacks and external disturbances.

III. Main Results

A. Observer and Controller Design

A decentralized state observer is proposed for estimating the system states:

$$\begin{aligned} \dot{\hat{x}}_i(t) &= A\hat{x}_i(t) + B\left[u_i(t) + \hat{d}_i(t)\right] + K_1(y_i(t) - \hat{y}_i(t)), \\ \hat{y}_i(t) &= C\hat{x}_i(t), \ i = 1, \cdots, M, \end{aligned} \tag{7}$$

Authorized licensed use limited to: STAATS U UNIBIBL BREMEN. Downloaded on March 16,2025 at 11:30:45 UTC from IEEE Xplore. Restrictions apply.

This article has been accepted for inclusion in a future issue of this journal. Content is final as presented, with the exception of pagination.

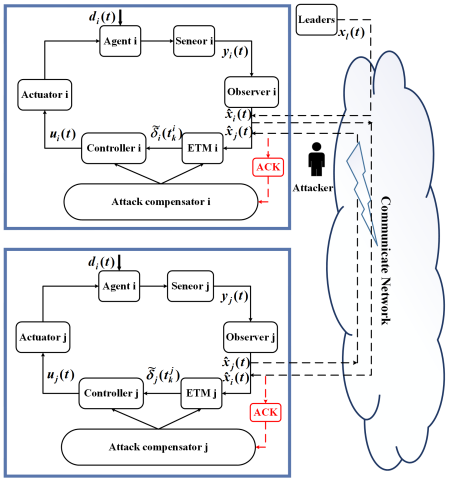


Fig. 2. The diagram of MASs under DoS attacks and external disturbances.

where $\hat{x}_i(t) \in \mathbb{R}^n$, $\hat{y}_i(t) \in \mathbb{R}^p$ are the estimated values of state $x_i(t)$ and output $y_i(t)$, respectively, $K_1 \in \mathbb{R}^{n\times p}$ is a state observer gain matrix.

A disturbance observer is designed to estimate the unknown disturbances as follows:

$$\begin{aligned}\dot{\hat{\omega}}_i(t) &= W\hat{\omega}_i(t) + F_1 f_{01}\left(\hat{\omega}_i(t)\right) + K_2(y_i(t) - \hat{y}_i(t)),\\ \hat{d}_i(t) &= V\hat{\omega}_i(t) + F_2 f_{02}\left(\hat{\omega}_i(t)\right),\ i = 1,\cdots,M,\end{aligned} \tag{8}$$

where $\hat{\omega}_i(t) \in \mathbb{R}^q$, $\hat{d}_i(t) \in \mathbb{R}^m$ are estimated states of the exogenous system, respectively, $K_2 \in \mathbb{R}^{q\times p}$ is a disturbance observer gain matrix.

Remark 3: The decentralized state observer and the disturbance observer are constructed in (7) and (8) based on the output information of the MASs. The basic idea is derived from the design of the extended state observer, which is then adapted to develop two observers for estimating unknown states and external disturbances.

Define the state estimation error and disturbance estimation error as $e_{x_i}(t) = x_i(t) - \hat{x}_i(t)$ and $e_{\omega_i}(t) = \omega_i(t) - \hat{\omega}_i(t)$, respectively. Suppose the leaders' reference signal can be available, i.e., $\hat{x}_l(t) = x_l(t)$, then the dynamic of $e_x(t)$ is

$$\begin{aligned}\dot{e}_x(t) &= [I_M \otimes (A - K_1C)]\, e_x(t) + (I_q \otimes BV)e_\omega(t)\\ &\quad + (I_M \otimes BF_2)\left[f_{02}(\omega(t)) - f_{02}(\hat{\omega}(t))\right],\end{aligned} \tag{9}$$

where $e_x(t) = \left[e_{x_1}^T(t), e_{x_2}^T(t), \cdots, e_{x_M}^T(t)\right]^T$, $f_{02}(\omega(t)) = \left[f_{02}(\omega_1(t)), \cdots, f_{02}(\omega_q(t))\right]^T$ and $f_{02}(\hat{\omega}(t)) = \left[f_{02}(\hat{\omega}_1(t)), \cdots, f_{02}(\hat{\omega}_q(t))\right]^T$.

The dynamic of the disturbance estimate error is given by:

$$\begin{aligned}\dot{e}_\omega(t) &= (I_q \otimes W)e_\omega(t) - (I_M \otimes K_2C)e_x(t)\\ &\quad + (I_q \otimes F_1)\left[f_{01}(\omega(t)) - f_{01}(\hat{\omega}(t))\right],\end{aligned} \tag{10}$$

where $e_\omega(t) = \left[e_{\omega_1}^T(t), e_{\omega_2}^T(t), \cdots, e_{\omega_q}^T(t)\right]^T$, $f_{01}(\omega(t)) = \left[f_{01}(\omega_1(t)), \cdots, f_{01}(\omega_q(t))\right]^T$ and $f_{01}(\hat{\omega}(t)) = \left[f_{01}(\hat{\omega}_1(t)), \cdots, f_{01}(\hat{\omega}_q(t))\right]^T$.

Denote the error vector as $\bar{e}_i(t) = \left[e_{x_i}(t), e_{\omega_i}(t)\right]^T$. The dynamic of $\bar{e}_i(t)$ is

$$\dot{\bar{e}}_i(t) = \left(\bar{A} - \bar{K}\bar{C}\right)\bar{e}_i(t) + \bar{F}\phi_i(t),\ i = 1,\cdots,M \tag{11}$$

with $\bar{A} = \begin{bmatrix} A & BV \\ \mathbf{0} & W\end{bmatrix}$, $\bar{K} = \begin{bmatrix} K_1 \\ K_2\end{bmatrix}$, $\bar{C} = \begin{bmatrix} C & \mathbf{0}\end{bmatrix}$, $\bar{F} = \begin{bmatrix} \mathbf{0} & BF_2 \\ F_1 & \mathbf{0}\end{bmatrix}$, $\phi_i(t) = \begin{bmatrix} f_{01}(\omega(t)) - f_{01}(\hat{\omega}(t)) \\ f_{02}(\omega(t)) - f_{02}(\hat{\omega}(t))\end{bmatrix}$, which can be simplified as

$$\dot{\bar{e}}(t) = \left(I_{M+q} \otimes (\bar{A} - \bar{K}\bar{C})\right)\bar{e}(t) + \left(I_{M+q} \otimes \bar{F}\right)\phi(t) \tag{12}$$

with $\bar{e}(t) = \left[\bar{e}_1^T(t), \bar{e}_2^T(t), \cdots, \bar{e}_M^T(t)\right]^T$.

When $\delta(ACK) = 0$ (i.e., no DoS attacks exist), the fully distributed control for i^{th} follower is constructed as follows:

$$\begin{aligned}u_i(t) &= -\hat{d}_i(t) + \alpha_{1i}(t)K_3\hat{\varepsilon}_i(t_k^i),\ i = 1,\cdots,M,\\ \dot{\alpha}_{1i}(t) &= \mathrm{Proj}_{[\underline{\alpha}_{1i},\overline{\alpha}_{1i}]}\{\alpha_{1i}(t)\}\\ &= \begin{cases} 0, & \text{if } \alpha_{1i}(t) = \overline{\alpha}_{1i} \text{ and } \Phi_{1i} > 0;\\ & \text{or } \alpha_{1i}(t) = \underline{\alpha}_{1i} \text{ and } \Phi_{1i} < 0;\\ \kappa_i\Phi_{1i}, & \text{otherwise,}\end{cases}\end{aligned} \tag{13}$$

where $\kappa_i > 0$, ∂_i is a positive constant, K_3, Γ are controller gain matrices, and $\Phi_{1i} = -\partial_i\alpha_{1i}(t) + \hat{\varepsilon}_i^T(t_k^i)\Gamma\hat{\varepsilon}_i(t_k^i)$, $\hat{\varepsilon}_i(t) = \sum_{h=1}^{M} a_{ih}\left(\hat{x}_i(t) - \mathrm{sgn}(a_{ih})\hat{x}_h(t)\right) + \sum_{l=M+1}^{N} a_{il}\left(\hat{x}_i(t) - \mathrm{sgn}(a_{il})x_l(t)\right)$. The Proj$\{*\}$ represents the projection operator [47]. To prevent excessive adaptive parameter, the projection operator is employed to constrain the adaptive parameter within a certain range, and this paper uses projection operation to project $\alpha_{1i}(t)$ to the scope of $[\underline{\alpha}_1(t), \overline{\alpha}_1(t)]$. Specifically, when $\alpha_{1i}(t)$ continues and reaches its maximum value $\overline{\alpha}_1(t)$, its rate of change $\dot{\alpha}_{1i}(t)$ resets to zero to prevent further growth. Similarly, when $\alpha_{1i}(t)$ decreases and reaches its minimum value $\underline{\alpha}_1(t)$, $\dot{\alpha}_{1i}(t)$ is also reset to zero to prevent further reduction. In other cases, $\alpha_{1i}(t)$ remains confined within the range $[\underline{\alpha}_1(t), \overline{\alpha}_1(t)]$ and evolves according to the rate of change of $\kappa_i\Phi_{1i}$.

The triggered instant time when $\delta(ACK) = 0$ is defined as $t_{k+1}^i = \inf\left\{t : g_{1i}(t) \geq 0, t > t_k^i\right\}$, in which the event-triggered function $g_{1i}(t)$ is

$$\begin{aligned}g_{1i}(t) &= \sigma_i\left[\alpha_{1i}(t)\|e_{\hat{\varepsilon}_i}(t)B^TQ_2^{-1}\|^2 - \|\hat{\varepsilon}_i(t_k^i)B^TQ_2^{-1}\|^2\right]\\ &\quad - \Upsilon_{1i}(t) \geq 0\end{aligned} \tag{14}$$

with the measurement error $e_{\hat{\varepsilon}_i}(t) = \hat{\varepsilon}_i(t_k^i) - \hat{\varepsilon}_i(t)$. $\Upsilon_i(t)$ is the dynamic internal variable:

$$\begin{aligned}\dot{\Upsilon}_{1i}(t) &= \sigma_i\left[\|\hat{\varepsilon}_i(t_k^i)B^TQ_2^{-1}\|^2 - \alpha_{1i}(t)\|e_{\hat{\varepsilon}_i}(t)B^TQ_2^{-1}\|^2\right]\\ &\quad - \rho_i\Upsilon_{1i}(t),\end{aligned} \tag{15}$$

where $\rho_i > 0$, $\sigma_i > 0$, $\Upsilon_{1i}(0) = \Upsilon_{i_0}$, $\Upsilon_{1i_0} \in \mathbb{R}^+$.

Remark 4: Considering the existence of the dynamic variables $\Upsilon_i(t)$ and $\alpha_{1i}(t)$, the trigger threshold is dynamically adjustable. Notably, compare to the dynamic ETM depend on global information in [44], the introduction of the adaptive parameter $\alpha_{1i}(t)$ in this paper eliminates the reliance on any global information, including topological structure information. Thus, the constructed dynamic ETM will not fail with the increase of the scale of communication topology.

The dynamics of followers and leaders can be simplified as

$$\begin{aligned}\dot{x}_F(t) &= (I_M \otimes A)\, x_F(t) + (\Psi_1(t) \otimes BK_3)\hat{\varepsilon}(t_k) + (I_q \otimes\\ &\quad BV)e_\omega(t) + (I_q \otimes BF_2)[f_{02}(\omega(t)) - f_{02}(\hat{\omega}(t))],\\ \dot{\hat{x}}_F(t) &= (I_M \otimes A)\,\hat{x}_F(t) + (\Psi_1(t) \otimes BK_3)\hat{\varepsilon}(t_k)\\ &\quad + (I_M \otimes K_1C)e_x(t),\\ \dot{x}_L(t) &= (I_{N-M} \otimes A)x_L(t),\end{aligned} \tag{16}$$

where $x_F(t) = \left[x_1^T(t), \ldots, x_M^T(t)\right]^T$, $\hat{x}_F(t) = \left[\hat{x}_1^T(t), \ldots, \hat{x}_M^T(t)\right]^T$, $x_L(t) = \left[x_{M+1}^T(t), \ldots, x_N^T(t)\right]^T$, $\hat{\varepsilon}(t_k) = \left[\hat{\varepsilon}_1^T(t_k), \cdots, \hat{\varepsilon}_M^T(t_k)\right]^T$, $\Psi_1(t) = \mathrm{diag}\{\alpha_{11}(t), \ldots, \alpha_{1M}(t)\}$.

Authorized licensed use limited to: STAATS U UNIBIBL BREMEN. Downloaded on March 16,2025 at 11:30:45 UTC from IEEE Xplore. Restrictions apply.

This article has been accepted for inclusion in a future issue of this journal. Content is final as presented, with the exception of pagination.

When $\delta(ACK)=1$ (i.e., DoS attacks exist), the dynamic equation $e(t)$ is

$$\dot{e}(t)=(I_M\otimes A)\,e(t)+(\Psi_1(t)\otimes BK_3)\hat{\varepsilon}(t_k)+(I_q\otimes BV)\times e_\omega(t)+(I_q\otimes BF_2)[f_{02}(\omega(t))-f_{02}(\hat{\omega}(t))]. \quad (17)$$

To reduce the influences of DoS attacks, a controller with an attack compensator when $\delta(ACK)=1$ is proposed:

$$\begin{aligned} u_i(t)&=-\hat{d}_i(t)+\alpha_{2i}(t)K_3\tilde{\varepsilon}_i(t_k^i),\ i=1,\cdots,M,\\ \dot{\alpha}_{2i}(t)&=\mathrm{Proj}_{[\underline{\alpha}_{2i},\overline{\alpha}_{2i}]}\{\alpha_{2i}(t)\}\\ &=\begin{cases}0, & \text{if } \alpha_{2i}(t)=\overline{\alpha}_{2i},\ \Phi_{2i}>0\\ & \text{or } \alpha_{2i}(t)=\underline{\alpha}_{2i},\ \Phi_{2i}<0;\\ \kappa_i\Phi_{2i}, & \text{otherwise};\end{cases}\end{aligned} \quad (18)$$

where $\Phi_{2i}=-\partial_i\alpha_{2i}(t)+\tilde{\varepsilon}_i^T(t_k^i)\Gamma\tilde{\varepsilon}_i(t_k^i)$, and $\tilde{\varepsilon}_i(t)=\sum_{h=1}^{M}a_{ih}\left(\hat{x}_i(t)-\mathrm{sgn}(a_{ih})\tilde{x}_h(t)\right)+\sum_{l=M+1}^{N}a_{il}\left(\hat{x}_i(t)-\mathrm{sgn}(a_{il})\tilde{x}_l(t)\right)$, which is formulated based on the reconstructed neighbor information by attack compensators.

The attack compensator is devised as follows:

$$\begin{cases}\dot{\tilde{x}}_h(t)=A\tilde{x}_h(t),\ t\in\left[T_n^{\mathrm{on}},T_n^{\mathrm{off}}\right)\\ \tilde{x}_h(t)=\hat{x}_h\left(t^-\right),\ t=T_n^{\mathrm{on}},\ h=1,\cdots,M,\\ \dot{\tilde{x}}_l(t)=A\tilde{x}_l(t),\ t\in\left[T_n^{\mathrm{on}},T_n^{\mathrm{off}}\right)\\ \tilde{x}_l(t)=x_l\left(t^-\right),\ t=T_n^{\mathrm{on}},\ l=M+1,\cdots,N.\end{cases} \quad (19)$$

Remark 5: The introduction of the ACK technology facilitates the detection of whether DoS attacks are occurring based on the reception of the ACK signal. Upon receiving error-free data, the controller provides a correct ACK signal (i.e., $\delta(ACK)=0$), indicates successful transmission and readiness for the next transmission. If a character error is detected, the attack compensator is activated until a correct ACK is received.

Remark 6: The presence of DoS attacks aims to disrupt communication between agents. Due to the unavailability of neighbor information, the control inputs for each agent will not achieve accurate real-time updates, thereby influencing system stability [32]. To mitigate the impact of DoS attacks, an open-loop observer is employed as an attack compensator. The compensator is simple in construction and relies only on the most recently received neighbor information and the known system model. Since agent i can predict its neighbors' states based on the attack compensator, it is reasonable to use the estimate $x_h(t)$ and $x_l(t)$ in the combinational states $\tilde{\varepsilon}_i(t)$ even though there is no continuous communication. The last estimated value is retained until the network transitions from an unreliable state to normal communication. Consequently, the compensator is activated only during finite period when DoS attacks occur.

Remark 7: The attack compensator primarily designed to enable agents to determine when to sample and broadcast the state information. The sampled state information is then utilized to construct the combinational states $\tilde{\varepsilon}_i(t)$. The use of the model provides estimates of the real states of neighboring agents, At the onset of the attack T_n^{on}, agent $j(j\in\mathcal{N}_i)$ transmits its current state $x_j(T_n^{\mathrm{on}})$ to its neighbors. The estimate $\tilde{x}_j(t)$ is updated continuously during the DoS attack interval and discretely at time instant $x_j(T_n^{\mathrm{on}})$.

Remark 8: In contrast to the compensator in [34], where all system states are estimated, including the states of both agents themselves and the neighboring agents, the open-loop compensator proposed in this paper is only used to estimate the states of the neighboring agents.

Remark 9: It should be noted that the select of parameters can significantly affect the system performance. The larger K_1/K_2, the faster $\hat{x}(t)/\hat{d}(t)$ approaches $x(t)/d(t)$, however, an excessively large K_1/K_2 can lead to system unstable. Notably, in practical system, sensors are often influenced by various noises. If observer gains are too large, noise effects can be amplified. In addition, as the control gain K_3 in the protocol increases, the system becomes more sensitive to errors, resulting in faster response speeds. Nevertheless, the excessively large control gains may lead to overshoot, thereby degrading the overall system performance.

The triggered instant time when $\delta(ACK)=1$ is defined as $t_{k+1}^i=\inf\left\{t:g_{2i}(t)\geq 0,t>t_k^i\right\}$, in which the event-triggered function $g_{2i}(t)$ is defined as:

$$g_{2i}(t)=\sigma_i\left[\alpha_{2i}(t)\|e_{\tilde{\varepsilon}_i}(t)B^TQ_2^{-1}\|^2-\|\tilde{\varepsilon}_i(t_k^i)B^TQ_2^{-1}\|^2\right]-\Upsilon_{2i}(t)\geq 0 \quad (20)$$

with measurement error $e_{\tilde{\varepsilon}_i}(t)=\tilde{\varepsilon}_i(t_k^i)-\tilde{\varepsilon}_i(t)$. $\Upsilon_{2i}(t)$ is the dynamic internal variable:

$$\dot{\Upsilon}_{2i}(t)=\sigma_i\left[\|\tilde{\varepsilon}_i(t_k^i)B^TQ_2^{-1}\|^2-\alpha_{2i}(t)\|e_{\tilde{\varepsilon}_i}(t)B^TQ_2^{-1}\|^2\right]-\rho_i\Upsilon_{2i}, \quad (21)$$

where $\rho_i>0$, $\sigma_i>0$, $\Upsilon_{2i}(0)=\Upsilon_{2i_0}$, $\Upsilon_{2i_0}\in\mathbb{R}^+$.

The dynamics of followers and leaders in $t\in[T_n^{\mathrm{on}},T_n^{\mathrm{off}})$ is

$$\begin{aligned}\dot{x}_F(t)&=(I_M\otimes A)\,x_F(t)+(\Psi_2(t)\otimes BK_3)\tilde{\varepsilon}(t_k)+(I_q\otimes BV)e_\omega(t)+(I_q\otimes BF_2)\left[f_{02}(\omega(t))-f_{02}(\hat{\omega}(t))\right],\\ \dot{\hat{x}}_F(t)&=(I_M\otimes A)\,\hat{x}_F(t)+(\Psi_2(t)\otimes BK_3)\tilde{\varepsilon}(t_k)+(I_M\otimes K_1C)e_x(t),\\ \dot{x}_L(t)&=(I_{N-M}\otimes A)x_L(t)\end{aligned} \quad (22)$$

with $\tilde{\varepsilon}(t_k)=\left[\tilde{\varepsilon}_1^T(t_k),\cdots,\tilde{\varepsilon}_M^T(t_k)\right]^T$, $\Psi_2(t)=\mathrm{diag}\{\alpha_{21}(t),\ldots,\alpha_{2M}(t)\}$.

The dynamic equation $e(t)$ can be obtained:

$$\dot{e}(t)=(I_M\otimes A)\,e(t)+(\Psi_2(t)\otimes BK_3)\tilde{\varepsilon}(t_k)+(I_q\otimes BV)\,e_\omega(t)+(I_q\otimes BF_2)\left[f_{02}(\omega(t))-f_{02}(\hat{\omega}(t))\right]. \quad (23)$$

Remark 10: According to the dynamic event-triggered conditions (14), it can be calculated that:

$$\sigma_i\left[\alpha_{1i}(t)\|e_{\hat{\varepsilon}_i}(t)B^TQ_2^{-1}\|^2-\|\hat{\varepsilon}_i(t_k^i)B^TQ_2^{-1}\|^2\right]<\Upsilon_{1i}(t),$$

then, we get

$$\dot{\Upsilon}_{1i}(t)>-(\rho_i+1)\Upsilon_{1i}(t). \quad (24)$$

By combining with comparison lemma, we can deduce that $\Upsilon_{1i}(t)>0,t>0$. Similarly, $\Upsilon_{2i}(t)>0,t>0$.

Remark 11: Compare with (14), the corresponding static event-triggered time instant $t_{k+1}^{i,s}$ is defined as $t_{k+1}^{i,s}=\inf\{t>t_k^{i,s}:\|\hat{\varepsilon}_i(t_k^i)B^TQ_2^{-1}\|^2-\alpha_{1i}(t)\|e_{\hat{\varepsilon}_i}(t)B^TQ_2^{-1}\|^2<0\}$. The inequality $t_{k+1}^{i,s}\leq t_{k+1}^{i,d}$ indicates that the next event-triggered time under the dynamic manner is larger than that in the static one, which can be analyzed by contradiction. Supposed that $t_{k+1}^{i,s}>t_{k+1}^{i,d}$. By the definition of $t_{k+1}^{i,s}$, we have $\|\hat{\varepsilon}_i(t_{k+1}^{i,d})B^TQ_2^{-1}\|^2-\alpha_{1i}(t)\|e_{\hat{\varepsilon}_i}(t)B^TQ_2^{-1}\|^2\geq 0$. When $t_{k+1}^{i,s}>0$, according to (14) and Remark 8, we obtain $\sigma_i\left[\|\hat{\varepsilon}_i(t_{k+1}^{i,d})B^TQ_2^{-1}\|^2-\alpha_{1i}(t)\|e_{\hat{\varepsilon}_i}(t)B^TQ_2^{-1}\|^2\right]\leq\sigma_i\left[\|\hat{\varepsilon}_i(t_{k+1}^{i,d})B^TQ_2^{-1}\|^2-\alpha_{1i}(t)\|e_{\hat{\varepsilon}_i}(t)B^TQ_2^{-1}\|^2\right]+\Upsilon_{1i}(t)<0$, which is contradicts with the previous inequality. Hence, we draw the conclusion $t_{k+1}^{i,s}\leq t_{k+1}^{i,d}$. A similar analysis can be

Authorized licensed use limited to: STAATS U UNIBIBL BREMEN. Downloaded on March 16,2025 at 11:30:45 UTC from IEEE Xplore. Restrictions apply.

This article has been accepted for inclusion in a future issue of this journal. Content is final as presented, with the exception of pagination.

performed for event-triggered conditions (20). Consequently, the number of triggers in the dynamic ETM is less than in the static framework, which can further conserving communication resources.

Remark 12: The variation of dynamic variables can be regulated using coefficients ρ_i and σ_i. Larger values of ρ_i and σ_i result in more frequent triggering events, which improve system performance but increase the communication burden. Conversely, smaller ρ_i and σ_i reduce the communication burden at the cost of system performance. Consequently, it is important to balance the relationship between communication burden and system performance.

Remark 13: The event-triggered mechanism activates sampling and control updates only when the triggering conditions are met, effectively reducing unnecessary data transmission and computation. However, the event-driven conditions rely on continuous-time supervision, which can increase the computational complexity, particularly in embedded or networked control systems, leading to additional processing overhead. Nevertheless, this overhead is often relatively small compared to the resource demands of communication, as energy consumption and bandwidth requirements for data transmission are more critical in many networked systems. Therefore, research has primarily focused on strategies to regulate the frequency of controller updates.

Remark 14: Unlike the existing secure bipartite tracking consensus results in [48], where the control protocol $u_i(t) = 0$ is applied during DoS attacks, the controller proposed in this paper still works even in the presence of such attacks and has good robust anti-disturbance performance. Furthermore, compared to the static ETM in [48], the introduction of a dynamic variable in our approach further reduces the number of triggers, thereby saves communication resources more efficiently.

B. Convergence Analysis of Estimation Errors

This part intends to discuss the convergence of estimation errors $e_x(t)$ and $e_w(t)$ under the designed state observer and disturbance observer.

Theorem 1: Consider the MASs (3)-(5) subjected to DoS attacks and external disturbances. For any constant $\check{\pi}$, if there is a matrix $Q_1 > 0$ such that

$$Q_1(\bar{A}-\bar{K}\bar{C})+(\bar{A}-\bar{K}\bar{C})^T Q_1+\frac{1}{\varrho_1}Q_1\bar{F}\bar{F}^T Q_1 + \check{\pi}\begin{pmatrix}\mathbf{0} & \mathbf{0}\\ \mathbf{0} & I_q\end{pmatrix}+Q_1<0. \tag{25}$$

Then, the state estimation errors $e_x(t)$ and disturbance estimate errors $e_\omega(t)$ tend to zero under the observers (7)-(8).

Proof: Choose Lyapunov function as $V_1(t) = \bar{e}^T(t)(L_1\otimes Q_1)\bar{e}(t)$. Calculating the derivative of $V_1(t)$ along the trajectories of (12) derives

$$\dot{V}_1(t)=\bar{e}^T(t)\left(L_1\otimes\left(Q_1(\bar{A}-\bar{K}\bar{C})+(\bar{A}-\bar{K}\bar{C})^T Q_1\right)\right)\bar{e}(t) + 2\bar{e}^T(t)\left(L_1\otimes Q_1\bar{F}\right)\phi(t). \tag{26}$$

According to Lemma 2, one yields

$$2\bar{e}^T(t)\left(L_1\otimes Q_1\bar{F}\right)\phi(t)\le\frac{1}{\varrho_1}\bar{e}^T(t)\left(L_1\otimes Q_1\bar{F}\bar{F}^T Q_1\right)\bar{e}(t) + \varrho_1\lambda_{\max}(L_1)\phi^T(t)\phi(t). \tag{27}$$

By using Assumption 3, it can be obtained

$$\begin{aligned}&\left[f_{01}(\omega(t))-f_{01}(\hat{\omega}(t))\right]^T\left[f_{01}(\omega(t))-f_{01}(\hat{\omega}(t))\right]\le\pi_1\|\omega(t)\\&\quad-\hat{\omega}(t)\|^2+\pi_2\langle f_{01}(\omega(t))-f_{01}(\hat{\omega}(t)),\omega(t)-\hat{\omega}(t)\rangle,\\&\langle f_{01}(\omega(t))-f_{01}(\hat{\omega}(t)),\omega(t)-\hat{\omega}(t)\rangle\le\pi_3\|\omega(t)-\hat{\omega}(t)\|^2,\\&\left[f_{02}(\omega(t))-f_{02}(\hat{\omega}(t))\right]^T\left[f_{02}(\omega(t))-f_{02}(\hat{\omega}(t))\right]\\&\le(\pi_4+\pi_5\pi_6)\|\omega(t)-\hat{\omega}(t)\|^2.\end{aligned} \tag{28}$$

Further, one has

$$\begin{aligned}&\left[\left[f_{01}(\omega(t))-f_{01}(\hat{\omega}(t))\right]^T\left[f_{02}(\omega(t))-f_{02}(\hat{\omega}(t))\right]^T\right]\\&\quad\times\begin{bmatrix}f_{01}(\omega(t))-f_{01}(\hat{\omega}(t))\\ f_{02}(\omega(t))-f_{02}(\hat{\omega}(t))\end{bmatrix}\varrho_1\lambda_{\max}(L_1)\\&\le\check{\pi}\bar{e}^T(t)\left(L_1\otimes\begin{pmatrix}\mathbf{0} & \mathbf{0}\\ \mathbf{0} & I_q\end{pmatrix}\right)\bar{e}(t)\end{aligned} \tag{29}$$

with $\check{\pi}=\frac{\varrho_1\lambda_{\max}(L_1)}{\lambda_{\min}(L_1)}(\pi_1+\pi_2\pi_3+\pi_4+\pi_5\pi_6)$. According to the above analysis, one can get

$$2\bar{e}^T(t)\left(L_1\otimes Q_1\bar{F}\right)\phi(t)\le\frac{1}{\varrho_1}\bar{e}^T(t)\left(L_1\otimes Q_1\bar{F}\bar{F}^T Q_1\right)\bar{e}(t) + \check{\pi}\bar{e}^T(t)\left(L_1\otimes\begin{pmatrix}\mathbf{0} & \mathbf{0}\\ \mathbf{0} & I_q\end{pmatrix}\right)\bar{e}(t). \tag{30}$$

By combining (27)-(30) with (26), one has

$$\begin{aligned}\dot{V}_1(t)\le{}&\bar{e}^T(t)\left(L_1\otimes\left(Q_1(\bar{A}-\bar{K}\bar{C})+(\bar{A}-\bar{K}\bar{C})^T Q_1\right)\right)\bar{e}(t)\\&+\frac{1}{\varrho_1}\bar{e}^T(t)\left(L_1\otimes Q_1\bar{F}\bar{F}^T Q_1\right)\bar{e}(t)\\&+\check{\pi}\bar{e}^T(t)\left(L_1\otimes\begin{pmatrix}\mathbf{0} & \mathbf{0}\\ \mathbf{0} & I_q\end{pmatrix}\right)\bar{e}(t).\end{aligned} \tag{31}$$

By combining with condition (25), it follows that

$$\dot{V}_1(t)<-\lambda_{\max}(Q_1)\bar{e}^T(t)(L_1\otimes I_M)\bar{e}(t). \tag{32}$$

Since L_1 is a positive definite matrix, then $\dot{V}_1(t)<0$. That is, $\bar{e}(t)\to 0$ along with $t\to\infty$. Therefore, the state estimation errors $e_x(t)$ and disturbance estimate errors $e_\omega(t)$ converge to zero along with $t\to\infty$, which demonstrates that the observers (7)-(8) can estimate both the system and external disturbances accurately. The proof is complete. ■

Remark 15: For the nonlinear term $f_{\mu 1}(\omega(t))-f_{\mu 2}(\hat{\omega}(t))$, the following inequality holds under the one-sided Lipschitz condition:

$$\langle f_{\mu 1}(\omega(t))-f_{\mu 2}(\hat{\omega}(t)),\omega(t)-\hat{\omega}(t)\rangle\le\gamma\|\omega(t)-\hat{\omega}(t)\|^2,$$

where γ is scalar. The one-sided Lipschitz condition is less conservative because the one-sided Lipschitz constant γ can take positive, zero, or even negative value, as compared to the positive constant in the corresponding Lipschitz condition.

C. Bipartite Containment Consensus Criterions

In this part, bipartite containment control criteria of the MAS (3)-(5) under the dynamic event-triggered strategy and attack compensator are established.

Theorem 2: The MASs (3)-(5) under DoS attacks and external disturbances can achieve bipartite containment control under the observers (7)-(8) and event-triggered-based controllers (13) and (18), if there is a matrix $Q_2>0$ satisfying

$$Q_2^{-1}A+A^T Q_2^{-1}-\eta_1 Q_2^{-1}BB^T Q_2^{-1}+\frac{1}{\iota_3}Q_2^{-1}BVV^T B^T Q_2^{-1} + \frac{1}{\varsigma}Q_2^{-1}BF_2F_2^T B^T Q_2^{-1}+\theta_1 Q_2^{-1}<0, \tag{33}$$

Authorized licensed use limited to: STAATS U UNIBIBL BREMEN. Downloaded on March 16,2025 at 11:30:45 UTC from IEEE Xplore. Restrictions apply.

This article has been accepted for inclusion in a future issue of this journal. Content is final as presented, with the exception of pagination.

$$Q_2^{-1}A + A^TQ_2^{-1} + \frac{\bar{\alpha}_2}{\iota_4}Q_2^{-1}BB^TQ_2^{-1} + \frac{1}{\iota_3}Q_2^{-1}BVV^TB^TQ_2^{-1} + \frac{1}{\varsigma}Q_2^{-1}BF_2F_2^TB^TQ_2^{-1} - \hat{\theta}_1Q_2^{-1} < 0, \tag{34}$$

$$\frac{\tilde{\zeta}_1 + \tilde{\zeta}_2}{\tilde{\zeta}_1} - \tau_a < 0, \tag{35}$$

where $\theta_1, \hat{\theta}_1, \eta_1, \iota_3, \iota_4, \varsigma$ are all positive constants, the feedback gain matrices are chosen as $K_3 = -B^TQ_2^{-1}$ and $\Gamma = Q_2^{-1}BB^TQ_2^{-1}$. Moreover, the adaptive parameters $\alpha_{1i}(t)$ and $\alpha_{2i}(t)$ are bounded.

Proof: If $\delta(ACK) = 0$, i.e., $t \in [T_{n-1}^{\text{off}}, T_n^{\text{on}})$, take Lyapunov function as $V_2(t) = e^T(t)\left(L_1 \otimes Q_2^{-1}\right)e(t) + \sum_{i=1}^{M}(1/\kappa_i)(\alpha_{1i}(t) - \vartheta)^2 + \sum_{i=1}^{M}\Upsilon_{1i}(t)$ with $\vartheta > 0$ to be given later.

Notably, there are two cases for $\dot{\alpha}_{1i}(t)$: when $\alpha_{1i}(t) = \bar{\alpha}_{1i}$ and $\Phi_{1i} > 0$ or $\alpha_{1i}(t) = \underline{\alpha}_{1i}$ and $\Phi_{1i} < 0$, we get $\sum_{i=1}^{M}(1/\kappa_i)(\alpha_{1i}(t) - \vartheta)\dot{\alpha}_{1i}(t) = 0$. In all other cases, $\sum_{i=1}^{M}(1/\kappa_i)(\alpha_{1i}(t) - \vartheta)\dot{\alpha}_{1i}(t) \neq 0$. Furthermore, only the latter case will be analysed, as it encompasses the former.

By taking the derivation of $V_2(t)$, one derive

$$\begin{aligned}\dot{V}_2(t) = {} & e^T(t)\left(L_1 \otimes (Q_2^{-1}A + A^TQ_2^{-1})\right)e(t) + 2e^T(t) \\ & \times \left(L_1\Psi_1(t) \otimes Q_2^{-1}BK_3\right)\hat{\varepsilon}(t_k) + 2e^T(t)(L_1 \\ & \otimes Q_2^{-1}BV\Big)e_\omega(t) + 2e^T(t)\left(L_1 \otimes Q_2^{-1}BF_2\right) \\ & \times \left[f_{02}(\omega(t)) - f_{02}(\hat{\omega}(t))\right] + 2\sum_{i=1}^{M}(\alpha_{1i}(t) - \vartheta) \\ & \times \left(-\partial_i\alpha_{1i}(t) + \hat{\varepsilon}_i^T(t_k^i)\Gamma\hat{\varepsilon}_i(t_k^i)\right) - \sum_{i=1}^{M}\rho_i\Upsilon_{1i}(t) \\ & + \sum_{i=1}^{M}\sigma_i\left[\|\hat{\varepsilon}_i(t_k^i)B^TQ_2^{-1}\|^2 - \alpha_{1i}(t)\|e_{\hat{\varepsilon}_i}(t)B^TQ_2^{-1}\|^2\right].\end{aligned} \tag{36}$$

According to the definition of $\hat{\varepsilon}_i(t)$, one has

$$\begin{aligned}\hat{\varepsilon}(t) &= (L_1 \otimes I_M)\hat{x}_F(t) + (SL_2 \otimes I_{N-M})x_L(t) \\ &= (L_1 \otimes I_M)x_F(t) + (SL_2 \otimes I_{N-M})x_L(t) \\ &\quad + (L_1 \otimes I_M)\hat{x}_F(t) - (L_1 \otimes I_M)x_F(t) \\ &= (L_1 \otimes I_M)\left[x_F(t) + \left(L_1^{-1}SL_2 \otimes I_{N-M}\right)x_L(t)\right] \\ &\quad - (L_1 \otimes I_M)e_x(t) = (L_1 \otimes I_M)(e(t) - e_x(t)).\end{aligned} \tag{37}$$

In light of $K_3 = -B^TQ_2^{-1}$, one can obtain

$$\begin{aligned}& 2\,e^T(t)\left(L_1\Psi_1(t) \otimes Q_2^{-1}BK_3\right)\hat{\varepsilon}(t_k) \\ &= 2\hat{\varepsilon}^T(t)\left(\Psi_1(t) \otimes Q_2^{-1}BK_3\right)\hat{\varepsilon}(t_k) \\ &\quad + 2e_x(t)^T\left(L_1\Psi_1(t) \otimes Q_2^{-1}BK_3\right)\hat{\varepsilon}(t_k) \\ &= 2\left(\hat{\varepsilon}(t_k) - e_{\hat{\varepsilon}}(t)\right)^T\left(\Psi_1(t) \otimes Q_2^{-1}BK_3\right)\hat{\varepsilon}(t_k) \\ &\quad + 2e_x(t)^T\left(L_1\Psi_1(t) \otimes Q_2^{-1}BK_3\right)\hat{\varepsilon}(t_k) \\ &= -2\hat{\varepsilon}(t_k)^T\left(\Psi_1(t) \otimes Q_2^{-1}BB^TQ_2^{-1}\right)\hat{\varepsilon}(t_k) \\ &\quad + 2e_{\hat{\varepsilon}}(t)^T\left(\Psi_1(t) \otimes Q_2^{-1}BB^TQ_2^{-1}\right)\hat{\varepsilon}(t_k) \\ &\quad - 2e_x(t)^T\left(L_1\Psi_1(t) \otimes Q_2^{-1}BB^TQ_2^{-1}\right)\hat{\varepsilon}(t_k).\end{aligned} \tag{38}$$

Using Young's inequality yields

$$\begin{aligned}& -2e_x^T(t)\left(L_1\Psi_1(t) \otimes Q_2^{-1}BB^TQ_2^{-1}\right)\hat{\varepsilon}(t_k) \\ &\le \frac{1}{\iota_1}e_x^T(t)\left(L_1\Psi_1(t) \otimes Q_2^{-1}BB^TQ_2^{-1}\right)e_x(t) \\ &\quad + \iota_1\hat{\varepsilon}^T(t_k)\left(L_1\Psi_1(t) \otimes Q_2^{-1}BB^TQ_2^{-1}\right)\hat{\varepsilon}(t_k), \\ & 2e_{\hat{\varepsilon}}(t)^T\left(\Psi_1(t) \otimes Q_2^{-1}BB^TQ_2^{-1}\right)\hat{\varepsilon}(t_k) \\ &\le \frac{1}{\iota_2}e_{\hat{\varepsilon}}(t)^T\left(\Psi_1(t) \otimes Q_2^{-1}BB^TQ_2^{-1}\right)e_{\hat{\varepsilon}}(t) \\ &\quad + \iota_2\hat{\varepsilon}(t_k)^T\left(\Psi_1(t) \otimes Q_2^{-1}BB^TQ_2^{-1}\right)\hat{\varepsilon}(t_k),\end{aligned} \tag{39}$$

and

$$\begin{aligned}& 2e^T(t)\left(L_1 \otimes Q_2^{-1}BV\right)e_\omega(t) \le \frac{1}{\iota_3}e^T(t)\Big(L_1 \otimes Q_2^{-1}BV \\ &\quad V^TB^TQ_2^{-1}\Big)e(t) + \iota_3e_\omega^T(t)\left(L_1 \otimes I_q\right)e_\omega(t), \\ & 2e^T(t)\left(L_1 \otimes Q_2^{-1}BF_2\right)\left[f_{02}(\omega(t)) - f_{02}(\hat{\omega}(t))\right] \\ &\le \frac{1}{\varsigma}e^T(t)\left(L_1 \otimes Q_2^{-1}BF_2F_2^TB^TQ_2^{-1}\right)e(t) \\ &\quad + \varsigma(\pi_4 + \pi_5\pi_6)\frac{\lambda_{\max}(L_1)}{\lambda_{\min}(L_1)}e_\omega^T(t)\left(L_1 \otimes I_q\right)e_\omega(t).\end{aligned} \tag{40}$$

Moreover, we make the following transformation:

$$\begin{aligned}& 2\sum_{i=1}^{M}(\alpha_{1i}(t) - \vartheta)(-\partial_i\alpha_{1i}(t)) < -\sum_{i=1}^{M}\partial_i\left(\alpha_{1i}^2(t) - 2\vartheta\alpha_{1i}(t)\right) \\ &= -\sum_{i=1}^{M}\partial_i(\alpha_{1i}(t) - \vartheta)^2 + \sum_{i=1}^{M}\partial_i\vartheta^2.\end{aligned} \tag{41}$$

Let $\Gamma = Q_2^{-1}BB^TQ_2^{-1}$. By substituting (38)-(41) into (36), one can deduce

$$\begin{aligned}\dot{V}_2(t) \le {} & e^T(t)\left(L_1 \otimes \left(Q_2^{-1}A + A^TQ_2^{-1}\right)\right)e(t) + \frac{1}{\iota_3}e^T(t) \\ & \times \left(L_1 \otimes Q_2^{-1}BVV^TB^TQ_2^{-1}\right)e(t) + \frac{1}{\varsigma}e^T(t) \\ & \times \left(L_1 \otimes Q_2^{-1}BF_2F_2^TB^TQ_2^{-1}\right)e(t) + \frac{1}{\iota_1}e_x^T(t) \\ & \times \left(L_1\Psi_1(t) \otimes Q_2^{-1}BB^TQ_2^{-1}\right)e_x(t) + \frac{1}{\iota_2}e_{\hat{\varepsilon}}^T(t) \\ & \times \left(\Psi_1(t) \otimes Q_2^{-1}BB^TQ_2^{-1}\right)e_{\hat{\varepsilon}}(t) + \sum_{i=1}^{M}\partial_i\vartheta^2 \\ & + (\iota_3 + \varsigma(\pi_4 + \pi_5\pi_6))e_\omega^T(t)\left(L_1 \otimes I_q\right)e_\omega(t) \\ & - \sum_{i=1}^{M}\rho_i\Upsilon_{1i}(t) - (2\vartheta - (\iota_1\lambda_{\max}(L_1) + \iota_2)\bar{\alpha}_1)\hat{\varepsilon}^T(t_k) \\ & \times \left(I_M \otimes Q_2^{-1}BB^TQ_2^{-1}\right)\hat{\varepsilon}(t_k) - \sum_{i=1}^{M}\partial_i(\alpha_{1i}(t) - \vartheta)^2 \\ & + \sum_{i=1}^{M}\sigma_i\left[\|\hat{\varepsilon}_i(t_k^i)B^TQ_2^{-1}\|^2 - \alpha_{1i}(t)\|e_{\hat{\varepsilon}_i}(t)B^TQ_2^{-1}\|^2\right]\end{aligned} \tag{42}$$

Authorized licensed use limited to: STAATS U UNIBIBL BREMEN. Downloaded on March 16,2025 at 11:30:45 UTC from IEEE Xplore. Restrictions apply.

This article has been accepted for inclusion in a future issue of this journal. Content is final as presented, with the exception of pagination.

with $\overline{\alpha}_1 = \max\{\alpha_{11}, \cdots, \alpha_{1M}\}$. Moreover, let $\hbar_1 = 2\vartheta - (\iota_1\lambda_{\max}(L_1) + \iota_2)\overline{\alpha}_1$. It is not difficult to get

$$\begin{aligned} &-\frac{\hbar_1}{2}\hat{\varepsilon}^T(t_k)\left(I_M \otimes Q_2^{-1}BB^TQ_2^{-1}\right)\hat{\varepsilon}(t_k) \\ &\le -\frac{\hbar_1}{4}\hat{\varepsilon}^T(t)\left(I_M \otimes Q_2^{-1}BB^TQ_2^{-1}\right)\hat{\varepsilon}(t) \\ &\quad + \frac{\hbar_1}{2}e_{\hat{\varepsilon}}^T(t)\left(I_M \otimes Q_2^{-1}BB^TQ_2^{-1}\right)e_{\hat{\varepsilon}}(t). \end{aligned} \tag{43}$$

Besides, one has

$$\begin{aligned} \hat{\varepsilon}^T(t)\left(I_M \otimes Q_2^{-1}BB^TQ_2^{-1}\right)\hat{\varepsilon}(t) &\le 2e^T(t)\left(L_1^TL_1 \otimes Q_2^{-1}BB^TQ_2^{-1}\right)e(t) \\ &\quad + 2e_x^T(t)\left(L_1^TL_1 \otimes Q_2^{-1}BB^TQ_2^{-1}\right)e_x(t). \end{aligned} \tag{44}$$

Substituting (43)-(44) into (42) leads to

$$\begin{aligned} \dot{V}_2(t) &\le e^T(t)\left(L_1 \otimes \left(Q_2^{-1}A + A^TQ_2^{-1}\right)\right)e(t) - \frac{\hbar_1}{2}e^T(t) \\ &\quad \times \left(L_1^TL_1 \otimes Q_2^{-1}BB^TQ_2^{-1}\right)e(t) + \frac{1}{\iota_3}e^T(t)\left(L_1\right. \\ &\quad \left.\otimes Q_2^{-1}BVV^TB^TQ_2^{-1}\right)e(t) + \frac{1}{\varsigma}e^T(t)\left(L_1\right. \\ &\quad \left.\otimes Q_2^{-1}BF_2F_2^TB^TQ_2^{-1}\right)e(t) + \frac{1}{\iota_1}e_x^T(t)\left(L_1\Psi_1(t)\right. \\ &\quad \left.\otimes Q_2^{-1}BB^TQ_2^{-1}\right)e_x(t) - \frac{\hbar_1}{2}e_x^T(t)\left(L_1^TL_1\right. \\ &\quad \left.\otimes Q_2^{-1}BB^TQ_2^{-1}\right)e_x(t) - \frac{\hbar_1}{2}\hat{\varepsilon}^T(t_k)\left(I_M \otimes Q_2^{-1}B\right. \\ &\quad \left.\times\ B^TQ_2^{-1}\right)\hat{\varepsilon}(t_k) + \sum_{i=1}^{M}\partial_i\vartheta^2 - \sum_{i=1}^{M}\partial_i\left(\alpha_{1i}(t) - \vartheta\right)^2 \\ &\quad + \left(\iota_3 + \varsigma(\pi_4 + \pi_5\pi_6)\right)e_\omega^T(t)\left(L_1 \otimes I_q\right)e_\omega(t) \\ &\quad + \frac{\hbar_1}{2}e_{\hat{\varepsilon}}^T(t)\left(\left(1 + \frac{2\overline{\alpha}_1}{\hbar_1\iota_2}\right)I \otimes Q_2^{-1}BB^TQ_2^{-1}\right)e_{\hat{\varepsilon}}(t) \\ &\quad - \sum_{i=1}^{M}\rho_i\Upsilon_{1i}(t) + \sum_{i=1}^{M}\sigma_i\left[\|\hat{\varepsilon}_i(t_k^i)B^TQ_2^{-1}\|^2 - \alpha_{1i}(t)\right. \\ &\quad \left.\times\|e_{\hat{\varepsilon}_i}(t)B^TQ_2^{-1}\|^2\right]. \end{aligned} \tag{45}$$

If we combine the condition (33) with selected ϑ as $\max\{\bar{\sigma} + \frac{1}{2}(\iota_1\lambda_{\max}(L_1) + \iota_2)\overline{\alpha}_1, \frac{\eta_1}{\lambda_{\min}(L_1)} + \frac{\overline{\alpha}_1}{2}(\iota_1\lambda_{\max}(L_1) + \iota_2)\} \le \vartheta \le \underline{\sigma}\underline{\alpha}_1 - \frac{\overline{\alpha}_1}{\iota_2} + \frac{\overline{\alpha}_1}{2}(\iota_1\lambda_{\max}(L_1) + \iota_2)$, $\underline{\sigma} = \min\{\sigma_1, \cdots, \sigma_M\}$, $\underline{\alpha}_1 = \min\{\alpha_{11}, \cdots, \alpha_{1M}\}$, the following inequality holds

$$\begin{aligned} \dot{V}_2(t) &\le -\theta_1e^T(t)\left(L_1 \otimes Q_2^{-1}\right)e(t) - \frac{\hbar_1}{2}e_x^T(t)\left(L_1^TL_1\right. \\ &\quad \left.\otimes Q_2^{-1}BB^TQ_2^{-1}\right)e_x(t) + \frac{1}{\iota_1}e_x^T(t)\left(L_1\Psi_1(t)\right. \\ &\quad \left.\otimes Q_2^{-1}BB^TQ_2^{-1}\right)e_x(t) - \sum_{i=1}^{M}\partial_i\left(\alpha_{1i}(t) - \vartheta\right)^2 \\ &\quad + \left(\iota_3 + \varsigma(\pi_4 + \pi_5\pi_6)\right)e_\omega^T(t)\left(L_1 \otimes I_q\right)e_\omega(t) \\ &\quad + \sum_{i=1}^{M}\partial_i\vartheta^2 - \sum_{i=1}^{M}\rho_i\Upsilon_{1i}(t). \end{aligned} \tag{46}$$

According to the proof of Theorem 1, we can know that the observer error system is asymptotically stable, and then $e_x(t)$, $e_\omega(t)$ is bounded. Let $\Delta_1 = \sup\{(\frac{1}{\iota_1} - \frac{\hbar_1}{2})e_x^T(t)\left(L_1^TL_1 \otimes Q_2^{-1}BB^TQ_2^{-1}\right)e_x(t), (\iota_3 + \varsigma(\pi_4 + \pi_5\pi_6))e_\omega^T(t)(L_1 \otimes I_q)e_\omega(t)\}$. It can be derived

$$\begin{aligned} \dot{V}_2(t) &\le -\theta_1e^T(t)\left(L_1 \otimes Q_2^{-1}\right)e(t) - \sum_{i=1}^{M}\partial_i\left(\alpha_{1i}(t) - \vartheta\right)^2 \\ &\quad - \sum_{i=1}^{M}\rho_i\Upsilon_{1i}(t) + \hat{\Delta}_1 \\ &\le -\tilde{\zeta}_1V_2(t) + \hat{\Delta}_1, \end{aligned} \tag{47}$$

where $\tilde{\zeta}_1 = \min\{\theta_1, \partial_i\kappa_i, \rho_i\}$, $\hat{\Delta}_1 = \Delta_1 + \sum_{i=1}^{M}\partial_i\vartheta^2$.

Multiplying $e^{\tilde{\zeta}_1t}$ and taking the integral from the both sides of (47) yield $\int_{T_{n-1}^{\text{off}}}^{t}\dot{V}_2(t)e^{\tilde{\zeta}_1t}dt \le -\int_{T_{n-1}^{\text{off}}}^{t}\tilde{\zeta}_1e^{\tilde{\zeta}_1t}V_2(t)dt + \int_{T_{n-1}^{\text{off}}}^{t}\hat{\Delta}_1e^{\tilde{\zeta}_1t}dt$. Then, one can get

$$V_2(t) \le V_2\left(T_{n-1}^{\text{off}}\right)e^{-\tilde{\zeta}_1\left(t - T_{n-1}^{\text{off}}\right)} + \int_{T_{n-1}^{\text{off}}}^{t}\hat{\Delta}_1dt. \tag{48}$$

If $\delta(ACK) = 0$, i.e., $t \in \left[T_n^{\text{on}}, T_n^{\text{off}}\right)$, take Lyapunov function as $V_2(t) = e^T(t)\left(L_1 \otimes Q_2^{-1}\right)e(t) + \sum_{i=1}^{M}(1/\kappa_i)\left(\alpha_{2i}(t) - \vartheta\right)^2 + \sum_{i=1}^{M}\Upsilon_{2i}(t)$. Similar to the previous discussion, we focus our analysis on the case where $\sum_{i=1}^{M}(1/\kappa_i)\left(\alpha_{2i}(t) - \vartheta\right)\dot{\alpha}_{2i}(t) \ne 0$.

By taking the derivation of $V_2(t)$, one derive

$$\begin{aligned} \dot{V}_2(t) &= e^T(t)\left(L_1 \otimes \left(Q_2^{-1}A + A^TQ_2^{-1}\right)\right)e(t) + 2e^T(t) \\ &\quad \times \left(L_1\Psi_2(t) \otimes Q_2^{-1}BK_3\right)\tilde{\varepsilon}(t_k) + 2e^T(t)\left(L_1\right. \\ &\quad \left.\otimes Q_2^{-1}BF_2\right)\left[f_{02}(\omega(t)) - f_{02}(\hat{\omega}(t))\right] - \sum_{i=1}^{M}\rho_i\Upsilon_{2i}(t) \\ &\quad + 2e^T(t)\left(L_1 \otimes Q_2^{-1}BV\right)e_\omega(t) + 2\sum_{i=1}^{M}\left(\alpha_{2i}(t) - \vartheta\right) \\ &\quad \times \left(-\partial_i\alpha_{2i}(t) + \tilde{\varepsilon}_i^T(t_k^i)\Gamma\tilde{\varepsilon}_i(t_k^i)\right) + \sum_{i=1}^{M}\sigma_i\left[\|\tilde{\varepsilon}_i(t_k^i)\right. \\ &\quad \left.\times\ B^TQ_2^{-1}\|^2 - \alpha_{2i}(t)\|e_{\tilde{\varepsilon}_i}(t)B^TQ_2^{-1}\|^2\right]. \end{aligned} \tag{49}$$

Using Young's inequality and letting $K_3 = -B^TQ_2^{-1}$ give rise to

$$\begin{aligned} &-2e^T(t)\left(L_1\Psi_2(t) \otimes Q_2^{-1}BB^TQ_2^{-1}\right)\tilde{\varepsilon}(t_k) \\ &\le \frac{1}{\iota_4}e^T(t)\left(L_1\Psi_2(t) \otimes Q_2^{-1}BB^TQ_2^{-1}\right)e(t) \\ &\quad + \iota_4\tilde{\varepsilon}^T(t_k)\left(L_1\Psi_2(t) \otimes Q_2^{-1}BB^TQ_2^{-1}\right)\tilde{\varepsilon}(t_k). \end{aligned} \tag{50}$$

Let $\hbar_2 = 2\vartheta - (2 + \iota_4\lambda_{\max}(L_1))\overline{\alpha}_2$, $\overline{\alpha}_2 = \max\{\alpha_{21}, \cdots, \alpha_{2M}\}$, and $\Gamma = Q_2^{-1}BB^TQ_2^{-1}$. One has

$$\begin{aligned} \dot{V}_2(t) &\le e^T(t)\left(L_1 \otimes \left(Q_2^{-1}A + A^TQ_2^{-1}\right)\right)e(t) + \frac{1}{\iota_4}e^T(t) \\ &\quad \times \left(L_1\Psi_2(t) \otimes Q_2^{-1}BB^TQ_2^{-1}\right)e(t) + \frac{1}{\iota_3}e^T(t) \\ &\quad \times \left(L_1 \otimes Q_2^{-1}BVV^TB^TQ_2^{-1}\right)e(t) + \frac{1}{\varsigma}e^T(t) \\ &\quad \times \left(L_1 \otimes Q_2^{-1}BF_2F_2^TB^TQ_2^{-1}\right)e(t) - \hbar_2\tilde{\varepsilon}^T(t_k) \\ &\quad \times \left(I_M \otimes Q_2^{-1}BB^TQ_2^{-1}\right)\tilde{\varepsilon}(t_k) - \sum_{i=1}^{M}\rho_i\Upsilon_{2i}(t) \end{aligned}$$

Authorized licensed use limited to: STAATS U UNIBIBL BREMEN. Downloaded on March 16,2025 at 11:30:45 UTC from IEEE Xplore. Restrictions apply.

This article has been accepted for inclusion in a future issue of this journal. Content is final as presented, with the exception of pagination.

$$+(\iota_3+\varsigma(\pi_4+\pi_5\pi_6))\,e_\omega^T(t)\left(L_1\otimes I_q\right)e_\omega(t)$$
$$+\sum_{i=1}^{M}(\alpha_{2i}(t)-\vartheta)\left(-\partial_i\alpha_{2i}(t)\right)+\sum_{i=1}^{M}\sigma_i\Big[\|\tilde{\varepsilon}_i(t_k^i)$$
$$\times B^TQ_2^{-1}\|^2-\alpha_{2i}(t)\|e_{\tilde{\varepsilon}_i}(t)B^TQ_2^{-1}\|^2\Big]. \tag{51}$$

Besides, one has

$$-\frac{\hbar_2}{2}\tilde{\varepsilon}^T(t_k)\left(I_M\otimes Q_2^{-1}BB^TQ_2^{-1}\right)\tilde{\varepsilon}(t_k)$$
$$\le-\frac{\hbar_2}{4}\tilde{\varepsilon}^T(t)\left(I_M\otimes Q_2^{-1}BB^TQ_2^{-1}\right)\tilde{\varepsilon}(t)$$
$$+\frac{\hbar_2}{2}e_{\tilde{\varepsilon}}^T(t)\left(I_M\otimes Q_2^{-1}BB^TQ_2^{-1}\right)e_{\tilde{\varepsilon}}(t). \tag{52}$$

If we combine the condition (34) with selected ϑ as $(2+\iota_4\lambda_{\max}(L_1))\frac{\overline{\alpha}_2}{2}+\overline{\sigma}\le\vartheta\le(2+\iota_4\lambda_{\max}(L_1))\frac{\overline{\alpha}_2}{2}+\underline{\sigma}\underline{\alpha}_2$, $\underline{\alpha}_2=\min\{\alpha_{21},\cdots,\alpha_{2M}\}$, the following inequality holds

$$\dot{V}_2(t)\le\hat{\theta}_1e^T(t)\left(L_1\otimes Q_2^{-1}\right)e(t)+(\iota_3+\varsigma(\pi_4+\pi_5\pi_6))$$
$$\times e_\omega^T(t)(L_1\otimes I_q)e_\omega(t)-\sum_{i=1}^{M}\partial_i\left(\alpha_{2i}(t)-\vartheta\right)^2$$
$$+\sum_{i=1}^{M}\partial_i\vartheta^2-\sum_{i=1}^{M}\rho_i\Upsilon_{2i}(t). \tag{53}$$

Moreover, we can easy to know $e_\omega(t)$ is bounded. Let $\Delta_2=\sup\{(\iota_3+\varsigma(\pi_4+\pi_5\pi_6))\,e_\omega^T(t)(L_1\otimes I_q)e_\omega(t)\}$. It attains

$$\dot{V}_2(t)\le\hat{\theta}_1e^T(t)\left(L_1\otimes Q_2^{-1}\right)e(t)-\sum_{i=1}^{M}\partial_i\left(\alpha_{2i}(t)-\vartheta\right)^2$$
$$-\sum_{i=1}^{M}\rho_i\Upsilon_{2i}(t)+\hat{\Delta}_2$$
$$\le\tilde{\zeta}_2V_2(t)+\hat{\Delta}_2, \tag{54}$$

where $\tilde{\zeta}_2=\max\{\hat{\theta}_1,-\partial_i\kappa_i,-\rho_i\}$, $\hat{\Delta}_2=\Delta_2+\sum_{i=1}^{M}\partial_i\vartheta^2$.

By multiplying both sides of (54) by $e^{-\tilde{\zeta}_2t}$ and then integrating, it follows

$$V_2(t)\le V_2\left(T_n^{\text{on}}\right)e^{\tilde{\zeta}_2(t-T_n^{\text{on}})}+\int_{T_n^{\text{on}}}^{t}\hat{\Delta}_2dt. \tag{55}$$

Analyzing two cases of DoS attacks and integrating equations (48) and (55) yields

$$V_2(t)\le\begin{cases}V_2\left(T_{n-1}^{\text{off}}\right)e^{-\tilde{\zeta}_1\left(t-T_{n-1}^{\text{off}}\right)}+\int_{T_{n-1}^{\text{off}}}^{\text{of}}\Delta dt,\\ \qquad t\in\left[T_{n-1}^{\text{off}},T_n^{\text{on}}\right),\\ V_2\left(T_n^{\text{on}}\right)e^{\tilde{\zeta}_2(t-T_n^{\text{on}})}+\int_{T_n^{\text{on}}}^{t}\Delta dt,\\ \qquad t\in\left[T_n^{\text{on}},T_n^{\text{off}}\right),\end{cases}$$

where $\Delta=\max\{\hat{\Delta}_1,\ \hat{\Delta}_2\}$.

For the case of $t\in\left[T_{n-1}^{\text{off}},T_n^{\text{on}}\right)$, one has

$$V_2(t)\le V_2\left(T_{n-1}^{\text{off}}\right)e^{-\tilde{\zeta}_1\left(t-T_{n-1}^{\text{off}}\right)}+\int_{T_{n-1}^{\text{off}}}^{t}\Delta dt$$
$$\le V_2\left(T_{n-1}^{\text{on}}\right)e^{\tilde{\zeta}_2\left(T_{n-1}^{\text{off}}-T_{n-1}^{\text{on}}\right)}e^{-\tilde{\zeta}_1\left(t-T_{n-1}^{\text{off}}\right)}$$
$$+\int_{T_{n-1}^{\text{off}}}^{t}\Delta dt+\int_{T_{n-1}^{\text{on}}}^{T_{n-1}^{\text{off}}}\Delta e^{-\tilde{\zeta}_1\left(t-T_{n-1}^{\text{off}}\right)}dt$$
$$\le\cdots$$
$$\le V_2(0)e^{-\tilde{\zeta}_1|\Omega_s(0,t)|}e^{\tilde{\zeta}_2|\Omega_a(0,t)|}$$
$$+\int_0^t\Delta e^{-\tilde{\zeta}_1|\Omega_s(0,t)|}e^{\tilde{\zeta}_2|\Omega_a(0,t)|}dt. \tag{56}$$

Similar to the case of $t\in\left[T_{n-1}^{\text{off}},T_n^{\text{on}}\right)$, we have the following inequality:

$$V_2(t)\le V_2\left(T_n^{\text{on}}\right)e^{\tilde{\zeta}_2(t-T_n^{\text{on}})}+\int_{T_n^{\text{on}}}^{t}\Delta dt$$
$$\le V_2\left(T_{n-1}^{\text{off}}\right)e^{-\tilde{\zeta}_1\left(T_n^{\text{on}}-T_{n-1}^{\text{off}}\right)}e^{\tilde{\zeta}_2(t-T_n^{\text{on}})}$$
$$+\int_{T_n^{\text{on}}}^{t}\Delta dt+\int_{T_{n-1}^{\text{off}}}^{T_n^{\text{on}}}\Delta e^{\tilde{\zeta}_2(t-T_n^{\text{on}})}dt$$
$$\le\cdots$$
$$\le V_2(0)e^{-\tilde{\zeta}_1|\Omega_s(0,t)|}e^{\tilde{\zeta}_2|\Omega_a(0,t)|}$$
$$+\int_0^t\Delta e^{-\tilde{\zeta}_1|\Omega_s(0,t)|}e^{\tilde{\zeta}_2|\Omega_a(0,t)|}dt. \tag{57}$$

It is easy to get $|\Omega_s(0,t)|=t-|\Omega_a(0,t)|$. Besides, based on Assumption 2, we have $|\Omega_a(0,t)|<\Omega_0+(t/\tau_a)$. Combining (56) with (57) gives

$$V_2(t)\le e^{-\tilde{\zeta}_1(t-|\Omega_a(0,t)|)}e^{\tilde{\zeta}_2|\Omega_a(0,t)|}V_2(0)$$
$$+\int_0^t\Delta e^{-\tilde{\zeta}_1(t-|\Omega_a(0,t)|)}e^{\tilde{\zeta}_2|\Omega_a(0,t)|}dt$$
$$\le e^{\left(\tilde{\zeta}_1+\tilde{\zeta}_2\right)\Omega_0}e^{-\left(\tilde{\zeta}_1-\frac{\tilde{\zeta}_1+\tilde{\zeta}_2}{\tau_a}\right)t}V_2(0)$$
$$+\int_0^t\Delta e^{\left(\tilde{\zeta}_1+\tilde{\zeta}_2\right)\Omega_0}e^{-\left(\tilde{\zeta}_1-\frac{\tilde{\zeta}_1+\tilde{\zeta}_2}{\tau_a}\right)t}dt. \tag{58}$$

According to condition (35) in Theorem 2, we can induce that $\tilde{\zeta}_1-\frac{\tilde{\zeta}_1+\tilde{\zeta}_2}{\tau_a}>0$. The inequality (58) indicates that $V_2(t)$ is uniformly bounded, which meaning the systems (2)-(4) can achieve bipartite containment control under the designed decentralized observers and fully distributed controllers. Moreover, adaptive parameters $\alpha_{1i}(t)$ satisfies the following inequality:

$$\frac{(\alpha_{1i}(t)-\vartheta)^2}{\kappa_i}\le V_2(t)\le\delta\Rightarrow\alpha_{1i}(t)\le\sqrt{\kappa_i\delta}+\vartheta, \tag{59}$$

where $\delta=\Delta e^{\left(\tilde{\zeta}_1+\tilde{\zeta}_2\right)\Omega_0}/(\tilde{\zeta}_1-\frac{\tilde{\zeta}_1+\tilde{\zeta}_2}{\tau_a})$. Furthermore, $\alpha_{2i}(t)$ is a similar derivation. Therefore, the adaptive parameters $\alpha_{1i}(t)$ and $\alpha_{2i}(t)$ converge to some finite steady-state values. ■

D. Exclusion of Zeno Behavior

Next, we give Theorem 3 to prove that the Zeno behavior can be excluded in dynamic ETMs.

Theorem 3: Under the fully distributed controller (13) and (18) for MASs (3)-(5), the dynamic ETMs (14) and (20) are Zeno-free.

Proof: We can proof this conclusion by contradiction, and we will discuss it in the subsequent two cases.

Case I: When $\delta(ACK)=0$, assuming that Zeno behavior happens. Thus, there exists at least one agent i satisfying $\lim_{k\to\infty}t_k^i=T$, where $T>0$ is a constant and $t_k^i<T$. Then take the derivative of $e_{\hat{\varepsilon}_i}(t)$ in interval $\left(t_k^i,t_{k+1}^i\right)$,

$$\frac{\mathrm{d}\left\|e_{\hat{\varepsilon}_i}(t)\right\|}{\mathrm{d}t}=\frac{e_{\hat{\varepsilon}_i}^T(t)\dot{e}_{\hat{\varepsilon}_i}(t)}{\left\|e_{\hat{\varepsilon}_i}(t)\right\|}$$
$$\le\left\|\dot{e}_{\hat{\varepsilon}_i}(t)\right\|=\left\|\dot{\hat{\varepsilon}}_i(t_k^i)-\dot{\hat{\varepsilon}}_i(t)\right\|=\left\|\dot{\hat{\varepsilon}}_i(t)\right\|$$

Authorized licensed use limited to: STAATS U UNIBIBL BREMEN. Downloaded on March 16,2025 at 11:30:45 UTC from IEEE Xplore. Restrictions apply.

This article has been accepted for inclusion in a future issue of this journal. Content is final as presented, with the exception of pagination.

$$
\begin{aligned}
&= \|A\hat{\varepsilon}_i(t) + BK_3\sum_{h=1}^{M} a_{ih}\left(\alpha_{1i}(t)\hat{\varepsilon}_i(t_k^i) - \mathrm{sgn}(a_{ih})\alpha_{1h}(t)\right.\\
&\left.\times\hat{\varepsilon}_h(t_k^h)\right) + K_1C\sum_{h=1}^{M} a_{ih}\left(e_{x_i}(t) - \mathrm{sgn}(a_{ih})e_{x_h}(t)\right)\\
&+ BK_3\sum_{l=M+1}^{N} a_{il}\hat{\varepsilon}_i(t_k^i) + K_1C\sum_{l=M+1}^{N} a_{il}e_{x_i}(t)\|\\
&\le \bar{\nu}_{1i}, \qquad (60)
\end{aligned}
$$

where $\bar{\nu}_{1i} = \sup_{0\le t<T}\left\{\|A\hat{\varepsilon}_i(t) + BK_3\sum_{h=1}^{N} a_{ih}\left(\alpha_{1i}(t)\times\right.\right.$ $\hat{\varepsilon}_i(t_k^i) - \mathrm{sgn}(a_{ih})\alpha_{1h}(t)\hat{\varepsilon}_h(t_k^h)\big) + K_1C\sum_{h=1}^{N} a_{ih}\left(e_{x_i}(t) - \mathrm{sgn}(a_{ih})e_{x_h}(t)\right) + BK_3\sum_{l=M+1}^{N} a_{il}\hat{\varepsilon}_i(t_k^i) + K_1C\sum_{l=M+1}^{N}$ $a_{il}e_{x_i}(t)\|\big\} > 0$. It can be concluded that $V_1(t) \le V(0)$ from Theorem 1, which implies that $e_{x_i}(t)$, $e_{\omega_i}(t)$ are all bounded. And we can deduce that $e_i(t), \alpha_{1i}, \alpha_{2i}, i = 1,\ldots,M$ are bounded form Theorem 2. Note that $\hat{\varepsilon}(t) = (L_1\otimes I_M)(e(t) - e_x(t))$ is bounded. Hence, $\|\hat{\varepsilon}_i(t)\|$ and $\|\hat{\varepsilon}_i(t_k^i)\|$ are all bounded. Then $\bar{\nu}_{1i}$ does exist. Suppose that a nonnegative function $\xi(t)$ satisfies

$$
\dot{\xi}(t) = \bar{\wp}_i, \quad \xi(0) = \left\|e_{\hat{\varepsilon}_i}(t_k^i)\right\| = 0. \qquad (61)
$$

By (60) and comparison principle of differential systems, one has $\left\|e_{\hat{\varepsilon}_i}(t)\right\| \le \xi\left(t - t_k^i\right)$, and $\xi(t) = \bar{\wp}_i t$ is the solution of (61). Noting $\Upsilon_i(t) \ge \Upsilon_i(0)\exp\left[-(1+\rho_i)t\right]$, one can get that if $\left\|e_{\hat{\varepsilon}_i}(t)\right\|^2 \le \frac{\Upsilon_i(0)}{\overline{\sigma\alpha}_1\|BQ_2^{-1}\|^2}e^{-(1+\rho_i)t}$, then $g_{1i}(t) \le 0$. Thus, the evolution time of $\xi^2\left(t - t_k^i\right)$ from 0 to $\frac{\Upsilon_i(0)}{\overline{\sigma\alpha}_1\|BQ_2^{-1}\|^2}e^{-(1+\rho_i)t}$, denoted as τ_k^i, can be regarded as the lower bound of $t_{k+1}^i - t_k^i$. That is, τ_k^i can be gotten from the following equation:

$$
\left(\bar{\wp}_i\tau_k^i\right)^2 = \frac{\Upsilon_i(0)}{\overline{\sigma\alpha}_1\|BQ_2^{-1}\|^2}\exp\left[-(1+\rho_i)\left(t_k^i + \tau_k^i\right)\right]. \qquad (62)
$$

Since $\tau_k^i \le t_{k+1}^i - t_k^i$ and $\lim_{k\to\infty} t_k^i = T$, a contradiction that $0 = \frac{\Upsilon_i(0)}{\overline{\sigma\alpha}_1\|BQ_2^{-1}\|^2}e^{-(1+\rho_i)T}$ can be deduced from (62) when $k\to\infty$. Hence Zeno phenomenon is excluded.

Case II: When $\delta(ACK) = 1$, the derivative of $e_{\tilde{\varepsilon}_i}(t)$ in interval $\left(t_k^i, t_{k+1}^i\right)$ is

$$
\begin{aligned}
&\frac{\mathrm{d}\left\|e_{\tilde{\varepsilon}_i}(t)\right\|}{\mathrm{d}t} = \frac{e_{\tilde{\varepsilon}_i}^T(t)\dot{e}_{\tilde{\varepsilon}_i}(t)}{\left\|e_{\tilde{\varepsilon}_i}(t)\right\|}\\
&\le \left\|\dot{e}_{\tilde{\varepsilon}_i}(t)\right\| = \left\|\dot{\tilde{\varepsilon}}_i(t_k^i) - \dot{\tilde{\varepsilon}}_i(t)\right\| = \left\|\dot{\tilde{\varepsilon}}_i(t)\right\|\\
&= \|A\tilde{\varepsilon}_i(t) + BK_3\sum_{k=1}^{N} a_{ik}\alpha_{2i}(t)\tilde{\varepsilon}_i(t_k^i) + K_1C\sum_{k=1}^{N} a_{ik}e_{x_i}(t)\|\\
&\le \bar{\nu}_{2i}, \qquad (63)
\end{aligned}
$$

where $\bar{\nu}_{2i} = \sup_{0\le t<T}\left\{A\tilde{\varepsilon}_i(t) + BK_3\sum_{k=1}^{N} a_{ik}\alpha_{2i}(t)\tilde{\varepsilon}_i(t_k^i) + K_1C\sum_{k=1}^{N} a_{ik}e_{x_i}(t)\right\} > 0$. On the basis of attack compensator (19) and Assumption 2, we can easily conclude that $\tilde{\varepsilon}_i(t)$ is bounded, $\tilde{\varepsilon}_i(t_k^i)$ is also bounded. Besides, $e_{x_i}(t)$ and $\alpha_{2i}(t)$ are bounded as declared in Case I. Then $\bar{\nu}_{2i}$ does exist.

Similar to the proof of case 1, we can deduce that Zeno phenomenon is excluded by contradiction. ■

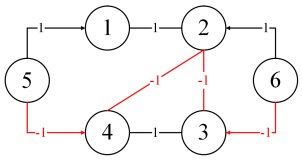


Fig. 3. Communication topology.

IV. Simulation Results and Analysis

This part utilizes a satellite flight system to validate the availability of the control scheme developed in this paper. Each satellite flying in low-Earth orbit is treated as an individual agent. It is assumed that there exist 6 agents, and their communication relationships are illustrated in Fig. 3. The black lines represent positive weights between agents, indicating cooperative relationships in their communication, whereas the red lines represent negative weights, representing competitive interactions among the agents. The weights between agents are ±1, respectively. The followers group is $\{1,2,3,4\}$, and the leaders group is $\{5,6\}$, Notably, the agents in followers group are structurally balanced and can be divided into $V_1 = \{1,2\}$ and $V_2 = \{3,4\}$.

The kinetic equation of the i^{th} satellite are given as follows:

$$
\begin{aligned}
\ddot{\hat{x}}_i - 2w_0\dot{\hat{y}}_i &= u_{xi} + d_{xi},\\
\ddot{\hat{y}}_i + 2w_0\dot{\hat{x}}_i - 3w_0^2\hat{y}_i &= u_{yi} + d_{yi},\\
\ddot{\hat{z}}_i + w_0^2\hat{z}_i &= u_{zi} + d_{zi}, \qquad (64)
\end{aligned}
$$

where $\hat{x}_i$, $\hat{y}_i$, $\hat{z}_i$ denote the position of the i-th satellite within the rotating coordinate frame, u_{xi}, u_{yi}, u_{zi} denote the control inputs, d_{xi}, d_{yi}, d_{zi} are external disturbances, ω_0 represents the angular rate of the virtual satellite. Denote the position vector $r_i = \left[\hat{x}_i\ \hat{y}_i\ \hat{z}_i\right]^T$, velocity vector $\dot{r}_i = \left[v_{xi}\ v_{yi}\ v_{zi}\right]^T$, control vector $u_i = \left[u_{xi}\ u_{yi}\ u_{zi}\right]^T$, disturbance vector $d_i = \left[d_{xi}\ d_{yi}\ d_{zi}\right]^T$. Satellite formation flying can be achieved if there exists a constant distance j_i satisfies $j_i - j_h \in \mathbb{R}^3$, such that $r_i - j_i \to r_h - j_h$, $\dot{r}_i \to \dot{r}_h$ for all $i,h \in \mathbb{N}$, where $j_i = \mathrm{col}(j_i^x,\ j_i^y,\ j_i^z)$. Let $\hat{r}_i = r_i - j_i$ and $x_i = \left[\hat{r}_i^T\ \dot{r}_i^T\right]^T$, it can be inferred from (64) that

$$
\dot{x}_i(t) = Ax_i(t) + B\left[u_i(t) + d_i(t)\right], i = 1,2,3,4,
$$

and the kinetic equation of virtul leader is

$$
\dot{x}_l(t) = Ax_l(t), l = 5,6
$$

with $A = [\mathbf{0}\ I_3; A_1\ A_2]$, $B = [\mathbf{0}; I_3]$, and

$$
A_1 = \begin{bmatrix} 0 & 0 & 0\\ 0 & 3w_0^2 & 0\\ 0 & 0 & -w_0^2 \end{bmatrix}, \quad A_2 = \begin{bmatrix} 0 & 2w_0 & 0\\ -2w_0 & 0 & 0\\ 0 & 0 & 0 \end{bmatrix},
$$

where $w_0 = 0.001$. The dynamics of external disturbances can be modeled as (4). Take matrices as $W = \begin{bmatrix} 0 & 1 & 0\\ -1 & 0 & 0\\ 0 & 0 & 0 \end{bmatrix}$, $V = \begin{bmatrix} 1 & 0 & 1\\ 0 & 1 & 0\\ 1 & 0 & 0 \end{bmatrix}$, $F_1 = \begin{bmatrix} 1 & 0 & 0\\ 0 & 1 & 0\\ 0 & 0 & 1 \end{bmatrix}$, $F_2 = \begin{bmatrix} 1 & 0 & 0\\ 0 & 1 & 0\\ 0 & 0 & 1 \end{bmatrix}$, and nonlinear functions $f_{01}(\omega_i(t)) = \left[0, 0, -\omega_{i1}(t)\left(\omega_{i1}^2(t) + \omega_{i3}^2(t)\right)\right]^T$, $f_{02}(\omega_i(t)) = \left[-\omega_{i2}(t)\left(\omega_{i1}^2(t) + \omega_{i3}^2(t)\right), 0, 0\right]^T$.

Select the initial states $x_1(0) = [0.5; -0.1; -0.5; 0.2; -0.11; 0.16]^T$, $x_2(0) = [-0.5; -0.12; -0.1; 0.5; 0.18; 0.2]^T$, $x_3(0) = [-0.9; 0.8; -0.3; 0.17; -0.2; 0.15]^T$, $x_4(0) = [0.14; -0.6; 0.5; -0.1; 0.18; -0.9]^T$, $x_5(0) = [-0.13; 0.1;$

Authorized licensed use limited to: STAATS U UNIBIBL BREMEN. Downloaded on March 16,2025 at 11:30:45 UTC from IEEE Xplore. Restrictions apply.

This article has been accepted for inclusion in a future issue of this journal. Content is final as presented, with the exception of pagination.

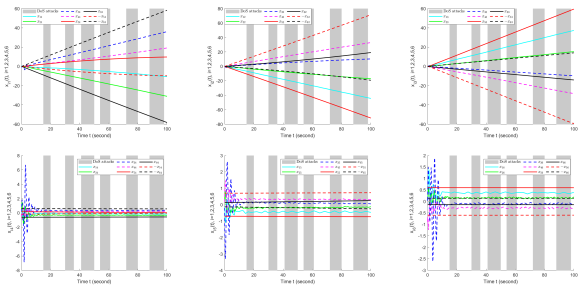


Fig. 4. Trajectories of agents.

TABLE I

NUMBERS OF TRIGGER OF EACH AGENT

	Agent 1	Agent 2	Agent 3	Agent 4	Total
$\rho_i = 4$	58	133	122	88	401
$\rho_i = 10$	80	167	193	124	564

$-0.4;\ 0.17; -0.7; 0.6]^T$, $x_6(0) = [0.1; 0.2; -0.1; -0.6; 0.13; -0.14]^T$. Assume that the total duration of DoS attacks as $t \in [15\text{s}, 20\text{s}] \cup [30\text{s}, 36\text{s}] \cup [41\text{s}, 50\text{s}] \cup [54\text{s}, 64\text{s}] \cup [72\text{s}, 80\text{s}] \cup [88\text{s}, 98\text{s}]$. Set parameters $\varrho_1 = 10, \breve{\pi} = -2.999, \eta_1 = 10, \iota_3 = 1, \iota_4 = 1, \varsigma = 1, \overline{\alpha}_1 = \overline{\alpha}_2 = 1, \theta_1 = 0.01, \hat{\theta}_1 = 100, \partial_1 = \partial_2 = \partial_3 = \partial_4 = \partial_5 = 1$, and event-triggered parameters $\rho_1 = \rho_2 = \rho_3 = \rho_4 = 4$, $\sigma_1 = \sigma_2 = \sigma_3 = \sigma_4 = 1$.

By solving the LMI, we obtain observers and controller gains as follows:

$$K_1 = \begin{bmatrix} 1.2177 & 0.0947 & 0.1377 \\ -0.0378 & 1.0380 & -0.0569 \\ 0.2218 & 0.0685 & 1.0117 \\ 7.2806 & 0.3487 & 1.2798 \\ -0.0562 & 5.8790 & -0.1770 \\ 1.3816 & 0.2612 & 5.7294 \end{bmatrix},$$

$$K_2 = \begin{bmatrix} 1.0688 & 1.2894 & 1.1420 \\ -0.7425 & 1.2349 & -1.0324 \\ 1.4303 & 0.2136 & -0.2656 \end{bmatrix}.$$

$$K_3 = \begin{bmatrix} -0.5682 & 0.0001 & 0.0142 & -2.5286 & 0 & 0.0561 \\ -0.0001 & -0.5821 & 0 & 0 & -2.5831 & 0 \\ 0.0142 & 0 & -0.5824 & 0.0561 & 0 & -2.5847 \end{bmatrix}.$$

Fig. 4 shows the trajectories of the six agents, where the red and black solid lines represent the trajectories of leaders 5 and 6, respectively, while the red and black dashed lines denote their symmetric trajectories. It can be observed that the trajectories of agents 1, 2 are contained within the scope surrounded by leaders' trajectories. Inversely, agents 3, 4 are contained in the opposite direction of the leaders' trajectories. This demonstrates that the agents can achieve bipartite containment under the designed fully distributed controller. Figs. 5 and 6 show curves of the states and disturbances estimations of followers. It demonstrates that the observers designed in this study can estimate both the system and external disturbances accurately. Fig. 7 presents the trajectories of the adaptive parameters $\alpha_i, i = 1, \cdots, 4$. Fig. 8 shows the event-triggered instants, which illustrates that the communication between agents is intermittent. Additionally, the trigger times under different parameters ρ_i are given in Table I. It demonstrates that the number of triggers increases if ρ_i increases.

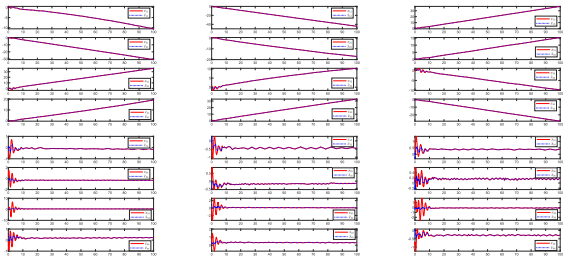


Fig. 5. Trajectories of followers and estimated states.

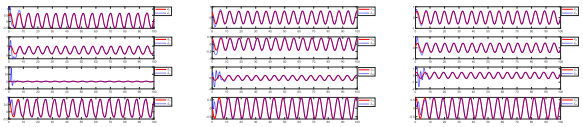


Fig. 6. Trajectories between disturbances and estimated states.

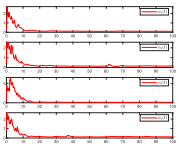


Fig. 7. Trajectories of adaptive parameter α_i.

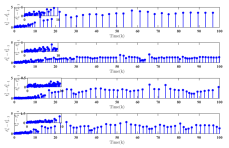


Fig. 8. Event release instants.

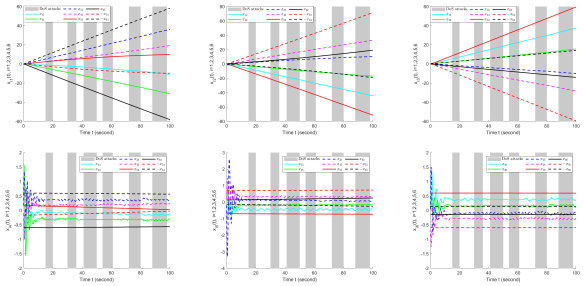


Fig. 9. Trajectories of agents with linear exogenous systems in Fig.1(a).

In addition, when the exogenous systems are modeled in linear form or Lipschitz nonlinear form, it can be seen from Figs. 9-10 that the system successfully achieves bipartite containment. This demonstrates that the controller proposed in this paper provides strong robustness of the system against different types of disturbances. Furthermore, Fig. 11 shows the state trajectories of the agents under persistent DoS attacks, highlighting the system's resilience performance under the proposed attack compensator.

Moreover, random white noises are considered to illustrate the impact of measurement noise on the observer performance. Figs. 12-13 show that the system's estimated performance degrade in the presence of random white noise, while still within acceptable thresholds.

A comparison simulation with the control scheme in literature [21] is done. In the absence of DoS attacks,

Authorized licensed use limited to: STAATS U UNIBIBL BREMEN. Downloaded on March 16,2025 at 11:30:45 UTC from IEEE Xplore. Restrictions apply.

This article has been accepted for inclusion in a future issue of this journal. Content is final as presented, with the exception of pagination.

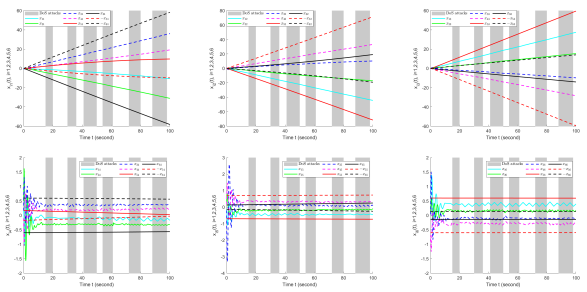


Fig. 10. Trajectories of agents with Lipschitz nonlinear exogenous systems in Fig.1(b).

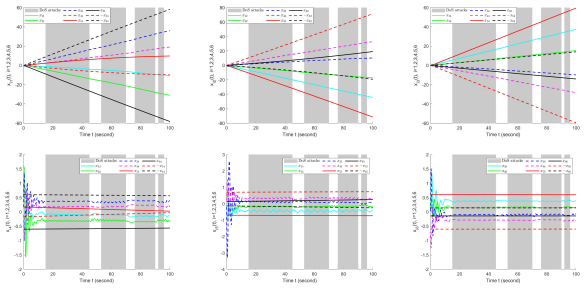


Fig. 11. Trajectories of agents under persistent DoS attacks.

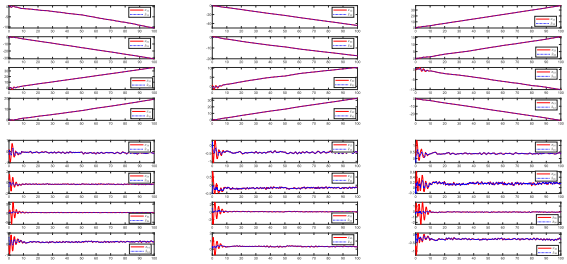


Fig. 12. Trajectories of followers and estimated states with random noises.

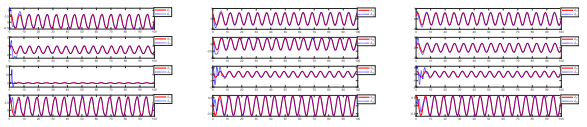


Fig. 13. Trajectories between disturbances and estimated states with random noises.

TABLE II

NUMBERS OF TRIGGER OF EACH AGENT

	Agent 1	Agent 2	Agent 3	Agent 4	Total
ETMs in (14)	57	141	172	97	467
ETMs in [21]	953	1864	1543	1511	5871

Figs. 14 and 15 show the system states trajectories. It can be observed that bipartite containment is achievable under both the controllers designed in this study and in [21]. However, the numbers of triggers in control scheme designed in this paper is less than that in [21], as shown in Table II. Fig. 16 demonstrates that under the control scheme designed in [21], the states of the agents become unbounded when DoS attacks and external disturbances coexist, whereas bipartite containment control can still be achieved under the control scheme based on observers and attack compensator designed in this paper.

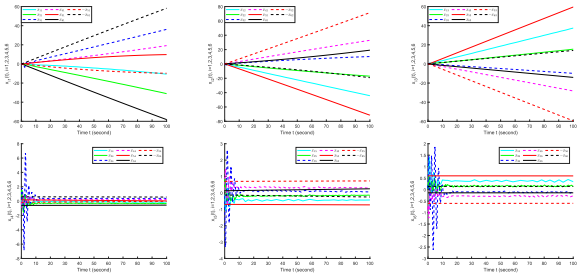


Fig. 14. Trajectories of agents under control scheme in this paper.

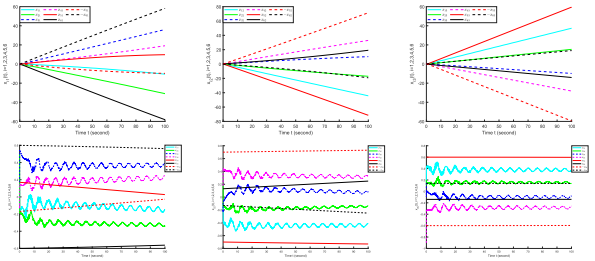


Fig. 15. Trajectories of agents under control scheme in [21].

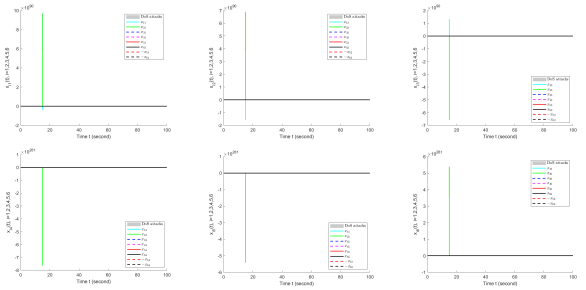


Fig. 16. Trajectories of agents under control scheme in [21].

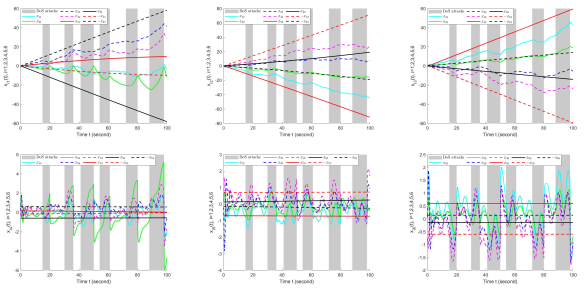


Fig. 17. Trajectories of agents under control scheme in [49].

Another simulation comparison of control performance with reference [49] is given in Fig. 17. As shown in Fig. 17, the control scheme proposed in [49] fails to achieve bipartite containment. In contrast, the control scheme proposed in this paper can achieve bipartite containment control well.

Furthermore, in comparison to the static ETM presented in [33], the dynamic ETMs designed in this paper exhibit fewer trigger times, as illustrated in Table III. In addition, the containment error obtained by using the proposed dynamic ETMs is smaller than that in [33], which can be observed in Table IV. This demonstrates that the ETMs developed in this paper represent a resource-efficient approach, while maintaining system performance.

Authorized licensed use limited to: STAATS U UNIBIBL BREMEN. Downloaded on March 16,2025 at 11:30:45 UTC from IEEE Xplore. Restrictions apply.

This article has been accepted for inclusion in a future issue of this journal. Content is final as presented, with the exception of pagination.

TABLE III
NUMBERS OF TRIGGER OF EACH AGENT

	Agent 1	Agent 2	Agent 3	Agent 4	Total
Dynamic ETMs	58	133	122	88	401
Static ETMs	137	300	288	223	948

TABLE IV
2-NORM OF CONTAINMENT ERRORS

	$\|e_1(t)\|_2$	$\|e_2(t)\|_2$	$\|e_3(t)\|_2$	$\|e_4(t)\|_2$
Dynamic ETMs	3067.18	6146.99	9921.65	14461.57
Static ETMs	3079.60	6178.29	9935.99	14478.94

V. CONCLUSION

This study has developed an event-triggered-based fully distributed control protocol to solve the bipartite containment problem of MASs affected by DoS attacks and exogenous disturbances. To estimate the unknown systems states and disturbances states, decentralized observers and disturbance observers have been introduced. Additionally, an attack compensator has been proposed to alleviate the effects of malicious attacks. For the propose of save limited communicate resources, dynamic ETMs have been presented, and the Zeno behavior has been excluded. Finally, satellite flight systems have been used to validate the effectiveness of the proposed control scheme. Future work will explore containment and bipartite containment control problems for MASs with communication delay, and focus particularly on ETMs to eliminate the need for the continuous-time supervision of event-driven conditions.

REFERENCES

[1] G. Zhao, L. Cui, and C. Hua, "Hybrid event-triggered bipartite consensus control of multiagent systems and application to satellite formation," *IEEE Trans. Autom. Sci. Eng.*, vol. 20, no. 3, pp. 1760–1771, Jun. 2022.

[2] Q. Yuan, Y. Wang, X. Liu, and Y. Lei, "Distributed fixed-time secondary control for DC microgrid via dynamic average consensus," *IEEE Trans. Sustain. Energy*, vol. 12, no. 4, pp. 2008–2018, Oct. 2021.

[3] M. Ji, G. Ferrari-Trecate, M. Egerstedt, and A. Buffa, "Containment control in mobile networks," *IEEE Trans. Autom. Control*, vol. 53, no. 8, pp. 1972–1975, Sep. 2008.

[4] S. J. Yoo, "Distributed adaptive containment control of uncertain nonlinear multi-agent systems in strict-feedback form," *Automatica*, vol. 49, no. 7, pp. 2145–2153, Jul. 2013.

[5] Y.-S. Ma, W.-W. Che, C. Deng, and Z.-G. Wu, "Observer-based event-triggered containment control for MASs under DoS attacks," *IEEE Trans. Cybern.*, vol. 52, no. 12, pp. 13156–13167, Dec. 2022.

[6] H. J. Kim and S. J. Yoo, "Adaptive fixed-time containment control of MIMO nonlinear multiagent systems via dynamic event-triggered communication," *Nonlinear Dyn.*, vol. 112, no. 13, pp. 11127–11145, Jul. 2024.

[7] C. Altafini, "Consensus problems on networks with antagonistic interactions," *IEEE Trans. Autom. Control*, vol. 58, no. 4, pp. 935–946, Apr. 2012.

[8] R. Sakthivel, A. Parivallal, F. Kong, and Y. Ren, "Bipartite consensus for Takagi–Sugeno fuzzy uncertain multi-agent systems with gain fluctuations," *IEEE Trans. Signal Inf. Process. Over Netw.*, vol. 9, pp. 74–83, Jan. 2023.

[9] S. Bhowmick and S. Panja, "Leader-follower bipartite consensus of linear multiagent systems over a signed directed graph," *IEEE Trans. Circuits Syst. II, Exp. Briefs*, vol. 66, no. 8, pp. 1436–1440, Aug. 2019.

[10] Y. Li, S. X. Ding, C. Hua, and G. Liu, "Distributed output-feedback bipartite consensus for stochastic nonlinear multiagent systems under directed switching networks," *IEEE Trans. Syst., Man, Cybern., Syst.*, vol. 53, no. 5, pp. 2748–2757, May 2023.

[11] Z.-H. Zhu, B. Hu, Z.-H. Guan, D.-X. Zhang, and T. Li, "Observer-based bipartite containment control for singular multi-agent systems over signed digraphs," *IEEE Trans. Circuits Syst. I, Reg. Papers*, vol. 68, no. 1, pp. 444–457, Jan. 2021.

[12] Y. Cai, H. Zhang, J. Duan, and J. Zhang, "Distributed bipartite consensus of linear multiagent systems based on event-triggered output feedback control scheme," *IEEE Trans. Syst., Man, Cybern., Syst.*, vol. 51, no. 11, pp. 6743–6756, Nov. 2021.

[13] R. Zhang, Y. Zhang, and X. Zong, "Bipartite containment of multi-leader multi-agent systems with antagonistic information and measurement noise," *IEEE Trans. Circuits Syst. I, Reg. Papers*, vol. 71, no. 9, pp. 4199–4210, Sep. 2024.

[14] Ž. Zečević, L. Martinović, and B. Krstajić, "Observer-based bipartite output containment control of heterogeneous multi-agent systems over structurally unbalanced signed graphs," *J. Franklin Inst.*, vol. 361, no. 14, Sep. 2024, Art. no. 107066.

[15] A. U. Rehman, M. Rehan, N. Iqbal, and C. K. Ahn, "Toward the LPV approach for adaptive distributed consensus of Lipschitz multi-agents," *IEEE Trans. Circuits Syst. II, Exp. Briefs*, vol. 66, no. 1, pp. 91–95, Jan. 2019.

[16] A. U. Rehman, M. Rehan, N. Iqbal, and C. K. Ahn, "LPV scheme for robust adaptive output feedback consensus of Lipschitz multiagents using Lipschitz nonlinear protocol," *IEEE Trans. Syst., Man, Cybern., Syst.*, vol. 51, no. 11, pp. 7040–7050, Nov. 2021.

[17] W. Xu, W. He, D. W. C. Ho, and J. Kurths, "Fully distributed observer-based consensus protocol: Adaptive dynamic event-triggered schemes," *Automatica*, vol. 139, May 2022, Art. no. 110188.

[18] K. Liu and Z. Ji, "Dynamic event-triggered consensus of general linear multi-agent systems with adaptive strategy," *IEEE Trans. Circuits Syst. II, Exp. Briefs*, vol. 69, no. 8, pp. 3440–3444, Aug. 2022.

[19] W. He, B. Xu, Q.-L. Han, and F. Qian, "Adaptive consensus control of linear multiagent systems with dynamic event-triggered strategies," *IEEE Trans. Cybern.*, vol. 50, no. 7, pp. 2996–3008, Jul. 2020.

[20] Y.-S. Ma, W.-W. Che, C. Deng, and Z.-G. Wu, "Observer-based fully distributed containment control for MASs subject to DoS attacks," *IEEE Trans. Syst., Man, Cybern., Syst.*, vol. 53, no. 2, pp. 897–907, Feb. 2023.

[21] J. Zhang, H. Zhang, W. Li, and Y. Wang, "Adaptive event-triggered bipartite containment control of linear multiagent systems under directed topologies," *IEEE Trans. Control Netw. Syst.*, vol. 10, no. 1, pp. 516–525, Mar. 2023.

[22] J. He, D. Yang, J. Zhang, and B. Zhou, "Fully distributed adaptive event-triggered bipartite containment control of linear multiagent systems with actuator faults," *Inf. Sci.*, vol. 677, Aug. 2024, Art. no. 120854.

[23] A. D. Syrmakesis, H. H. Alhelou, and N. D. Hatziargyriou, "Novel SMO-based detection and isolation of false data injection attacks against frequency control systems," *IEEE Trans. Power Syst.*, vol. 39, no. 1, pp. 1434–1446, Jan. 2023.

[24] K. Kumar, P. Kumar, S. Kar, and A. K. Bohre, "Anomaly detection technique for securing microgrid against false data attacks," *ISA Trans.*, vol. 153, pp. 13–27, Oct. 2024.

[25] C. Peng and H. Sun, "Switching-like event-triggered control for networked control systems under malicious denial of service attacks," *IEEE Trans. Autom. Control*, vol. 65, no. 9, pp. 3943–3949, Sep. 2020.

[26] R. Kato, A. Cetinkaya, and H. Ishii, "Linearization-based quantized stabilization of nonlinear systems under DoS attacks," *IEEE Trans. Autom. Control*, vol. 67, no. 12, pp. 6826–6833, Dec. 2022.

[27] D. Li, Q. Cai, D. Marelli, W. Meng, and M. Fu, "Stabilization of networked switched systems under DoS attacks," *IEEE Trans. Cybern.*, vol. 54, no. 8, pp. 4859–4866, Aug. 2024.

[28] Y. Xu, "Resilient secure control of networked systems over unreliable communication networks," *IEEE Trans. Ind. Informat.*, vol. 18, no. 6, pp. 4069–4077, Jun. 2022.

[29] M. A. Ali, M. Rehan, N. Iqbal, A. Basit, and C. K. Ahn, "A fully-distributed resilient dynamic output feedback consensus control for MASs under Markovian DoS attacks," *IEEE Trans. Autom. Sci. Eng.*, early access, Apr. 10, 2024, doi: 10.1109/TASE.2024.3385489.

[30] I. Ahmed, M. Rehan, A. Basit, F. S. Al-Ismail, and M. Khalid, "Consensus and clustering approach for dynamic event-triggered distributed optimization of power system networks with saturation constraint approche de consensus et de regroupement pour," *IEEE Can. J. Electr. Comput. Eng.*, vol. 47, no. 3, pp. 136–147, Mar. 2024.

[31] J. Y. Ko, J. M. Pak, D. H. Kim, and C. K. Ahn, "Secure event-triggered distributed finite-memory localization for multiple mobile robots under cyberattacks," *IEEE Trans. Ind. Electron.*, vol. 71, no. 10, pp. 12931–12941, Oct. 2024.

[32] D. V. Dimarogonas, E. Frazzoli, and K. H. Johansson, "Distributed event-triggered control for multi-agent systems," *IEEE Trans. Autom. Control*, vol. 57, no. 5, pp. 1291–1297, Jun. 2011.

Authorized licensed use limited to: STAATS U UNIBIBL BREMEN. Downloaded on March 16,2025 at 11:30:45 UTC from IEEE Xplore. Restrictions apply.

This article has been accepted for inclusion in a future issue of this journal. Content is final as presented, with the exception of pagination.

[33] W. Li, H. Zhang, Y. Cai, and Y. Wang, "Fully distributed event-triggered bipartite formation tracking for multi-agent systems with multiple leaders and matched uncertainties," *Inf. Sci.*, vol. 596, pp. 537–550, Jun. 2022.
[34] Y. Yang, Y. Li, D. Yue, Y.-C. Tian, and X. Ding, "Distributed secure consensus control with event-triggering for multiagent systems under DoS attacks," *IEEE Trans. Cybern.*, vol. 51, no. 6, pp. 2916–2928, Jun. 2021.
[35] M. Mousavian and H. Atrianfar, "Resilient event-triggered containment control of multi-agent systems under asynchronous DoS attacks and disturbances," *IEEE Trans. Control Netw. Syst.*, early access, Jul. 24, 2024, doi: 10.1109/TCNS.2024.3432951.
[36] M. Mousavian and H. Atrianfar, "Resilient adaptive event-triggered containment control of nonlinear multi-agent system under concurrent DoS attacks and disturbances," *Int. J. Syst. Sci.*, vol. 56, no. 1, pp. 40–59, Jan. 2025.
[37] Y. Wan, J. Cao, G. Chen, and W. Huang, "Distributed observer-based cyber-security control of complex dynamical networks," *IEEE Trans. Circuits Syst. I, Reg. Papers*, vol. 64, no. 11, pp. 2966–2975, Nov. 2017.
[38] H. Liang, X. Guo, Y. Pan, and T. Huang, "Event-triggered fuzzy bipartite tracking control for network systems based on distributed reduced-order observers," *IEEE Trans. Fuzzy Syst.*, vol. 29, no. 6, pp. 1601–1614, Jun. 2021.
[39] Q. Zhou, W. Wang, H. Liang, M. V. Basin, and B. Wang, "Observer-based event-triggered fuzzy adaptive bipartite containment control of multiagent systems with input quantization," *IEEE Trans. Fuzzy Syst.*, vol. 29, no. 2, pp. 372–384, Feb. 2021.
[40] Z.-G. Wu, Y. Xu, Y.-J. Pan, H. Su, and Y. Tang, "Event-triggered control for consensus problem in multi-agent systems with quantized relative state measurements and external disturbance," *IEEE Trans. Circuits Syst. I, Reg. Papers*, vol. 65, no. 7, pp. 2232–2242, Jul. 2018.
[41] T. Han, Z.-H. Guan, B. Xiao, and H. Yan, "Bipartite average tracking for multi-agent systems with disturbances: Finite-time and fixed-time convergence," *IEEE Trans. Circuits Syst. I, Reg. Papers*, vol. 68, no. 10, pp. 4393–4402, Oct. 2021.
[42] Q. Wang, W. He, L. Zino, D. Tan, and W. Zhong, "Bipartite consensus for a class of nonlinear multi-agent systems under switching topologies: A disturbance observer-based approach," *Neurocomputing*, vol. 488, pp. 130–143, Jun. 2022.
[43] Y. Luo, X. Gao, J. Cao, and A. Kashkynbayev, "Finite-time consensus for second-order leader-following multi-agent systems with external disturbances and internal nonlinear dynamics based on event-triggered pinning strategy," *Int. J. Robust Nonlinear Control*, vol. 32, no. 15, pp. 8558–8575, Oct. 2022.
[44] X. Guo, D. Zhang, J. Wang, J. Park, and L. Guo, "Observer-based event-triggered composite anti-disturbance control for multi-agent systems under multiple disturbances and stochastic FDIAs," *IEEE Trans. Autom. Sci. Eng.*, vol. 20, no. 1, pp. 528–540, Mar. 31, 2022.
[45] C. De Persis and P. Tesi, "Input-to-state stabilizing control under denial-of-service," *IEEE Trans. Autom. Control*, vol. 60, no. 11, pp. 2930–2944, Nov. 2015.
[46] X. Wang and J. H. Park, "State-based dynamic event-triggered observer for one-sided Lipschitz nonlinear systems with disturbances," *IEEE Trans. Circuits Syst. II, Exp. Briefs*, vol. 69, no. 4, pp. 2326–2330, Apr. 2022.
[47] P. A. Ioannou and J. Sun, *Robust Adaptive Control*. Englewood, CO, USA: Prentice-Hall, 2012.
[48] M. Cong, X. Mu, and Z. Hu, "Sampled-data-based event-triggered secure bipartite tracking consensus of linear multi-agent systems under DoS attacks," *J. Franklin Inst.*, vol. 358, no. 13, pp. 6798–6817, Sep. 2021.
[49] Z. Liu, H. Zhang, and Z. Wang, "Bipartite containment control of multi-agent systems under DoS attacks: An event-triggered scheme," *Int. J. Robust Nonlinear Control*, vol. 35, no. 2, pp. 479–495, Jan. 2025.



Yanjun Zhao received the M.S. degree in mathematics from Qufu Normal University, Qufu, China, in 2022. She is currently pursuing the Ph.D. degree in control science and engineering with the School of Engineering, Qufu Normal University, Rizhao, China.

Her research interests include consensus and containment control of multiagent systems.

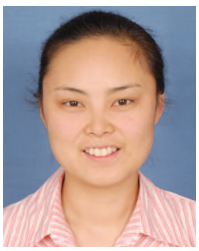


Haibin Sun (Member, IEEE) received the M.S. degree in operational research and cybernetics from the Institute of Automation, Qufu Normal University, Qufu, China, in 2009, and the Ph.D. degree in control theory and control engineering from the School of Automation, Southeast University, Nanjing, China, in 2013.

From March 2017 to January 2018, he was a Visiting Scholar with the School of Engineering, RMIT University, Melbourne, VIC, Australia. He was a Visiting Scholar with the School of Electrical and Electronic Engineering, Nanyang Technological University, Singapore, from July 2019 to September 2019. He is currently a Professor with the School of Engineering, Qufu Normal University. His main research interests include adaptive control, event-triggered control, and anti-disturbance control. He received the Title of Taishan Scholar in 2023.



Jun Yang (Fellow, IEEE) received the B.Sc. degree in automation from the Department of Automatic Control, Northeastern University, Shenyang, China, in 2006, and the Ph.D. degree in control theory and control engineering from the School of Automation, Southeast University, Nanjing, China, in 2011. He joined the Department of Aeronautical and Automotive Engineering, Loughborough University, in 2020, as a Senior Lecturer. His research interests include disturbance observer, motion control, visual servoing, nonlinear control, and autonomous systems. He is a fellow of IET and AAIA. He was a recipient of the EPSRC New Investigator Award. He serves as an Associate Editor or a Technical Editor for IEEE TRANSACTIONS ON INDUSTRIAL ELECTRONICS, IEEE/ASME TRANSACTIONS ON MECHATRONICS, IEEE OPEN JOURNAL OF INDUSTRIAL ELECTRONICS SOCIETY.



Linlin Hou was born in 1982. She received the B.S., M.S., and Ph.D. degrees in mathematics from Qufu Normal University, in 2006, 2009, and 2012, respectively. Since 2012, she has been with the School of Information Science and Engineering, Qufu Normal University, where she is currently a Professor. Her main research interests include stability, control, and robustness analysis of switched systems, and Markovian jump systems.



Dong Yang (Member, IEEE) received the M.S. degree in mathematics from the College of Engineering, Qufu Normal University, Qufu, China, in 2010, and the Ph.D. degree in control theory and control engineering from the College of Information Science and Engineering, Northeastern University, Shenyang, China, in 2017.

In 2020, he was a Senior Research Assistant with the Department of Electrical and Electronic Engineering, The University of Hong Kong, Hong Kong, SAR, China. In 2021, he was a Post-Doctoral Fellow with the Department of Electrical and Electronic Engineering, The University of Hong Kong. He is currently a Professor with the School of Engineering, Qufu Normal University. His research interests include Markovian jump systems, switched LPV systems, switched systems, bumpless transfer, H_∞ control, and their applications.

Authorized licensed use limited to: STAATS U UNIBIBL BREMEN. Downloaded on March 16,2025 at 11:30:45 UTC from IEEE Xplore. Restrictions apply.